

α_2 -Adrenoceptor Antagonists: Synthesis, Pharmacological Evaluation, and Molecular Modeling Investigation of Pyridinoguanidine, Pyridino-2-aminoimidazoline and Their Derivatives

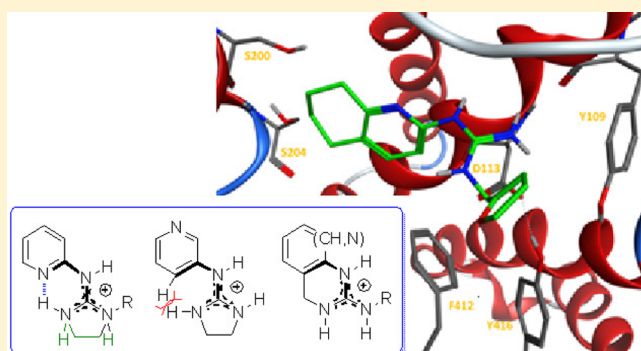
Brendan Kelly,[†] Michela McMullan,[†] Carolina Muguruza,[‡] Jorge E. Ortega,[‡] J. Javier Meana,[‡] Luis F. Callado,[‡] and Isabel Rozas^{*,†}

[†]School of Chemistry, Trinity Biomedical Sciences Institute, Trinity College Dublin, 152-160 Pearse Street, Dublin 2, Ireland

[‡]Department of Pharmacology, University of the Basque Country UPV/EHU, and Centro de Investigación Biomédica en Red de Salud Mental, CIBERSAM, 28029 Madrid, Spain

S Supporting Information

ABSTRACT: We have previously identified phenylguanidine and phenyl-2-aminoimidazoline compounds as high affinity ligands with conflicting functional activity at the α_2 -adrenoceptor, a G-protein-coupled receptor with relevance in several neuropsychiatric conditions. In this paper we describe the design, synthesis, and pharmacological evaluation of a new series of pyridine derivatives [para substituted 2- and 3-guanidino and 2- and 3-(2-aminoimidazolino)pyridines, disubstituted 2-guanidinopyridines and N-substituted-2-amino-1,4-dihydroquinazolines] that were found to be antagonists/inverse agonists of the α_2 -adrenoceptor. Furthermore, the compounds exert their effects at the α_2 -adrenoceptor both in vitro in human prefrontal cortex tissue and in vivo in rat brain as shown by microdialysis experiments. We also provide a docking study at the α_{2A} - and α_{2C} -adrenoceptor subtypes demonstrating the structural features required for high affinity binding to the receptor.



INTRODUCTION

The burden of mental health conditions is on the rise globally, and they are the second leading cause of disability worldwide, surpassing all cancers combined and being outranked only by cardiovascular diseases.¹ For many, the symptoms of depression, schizophrenia, or bipolar disorder can be treated with current medications; however, a substantial proportion of patients obtain no improvements with these treatments.

Two of the most important neuropsychiatric disorders, depression and schizophrenia, have been linked to the noradrenergic function in the brain. Pathophysiologically, depression is characterized by reduced monoamine activity (particularly noradrenaline (NA) and serotonin) in the brain, and correcting this imbalance has been the approach of all currently marketed antidepressants. Depression is associated with increased density of the α_2 -adrenoceptors (α_2 -ARs) in the brain as well as a selective increase in the high-affinity conformation of the α_2 -ARs.² Moreover, the dorsolateral prefrontal cortex (DLPFC) is the main anatomical pathway for the cognitive symptoms of schizophrenia, and the postsynaptic α_{2C} -ARs located on the DLPFC cells control the noradrenergic tone that maintains the basal cognitive activity. Either too little or too much NA impairs DLPFC function.

Therefore, α_2 -AR antagonists, which increase the release of NA and also potentiate dopamine release in the prefrontal cortex (PFC),^{3,4} seem useful pharmacological tools for the treatment of depression (α_2 -AR antagonists) and schizophrenia (selective α_{2C} -AR antagonists). Thus, the development of selective α_2 -AR antagonists suitable for clinical use can be considered as an effective approach to the treatment of neuropsychiatric disorders. For example, one of the most recent antidepressants marketed is mirtazapine, which shows effective activity by blockade of α_{2A} - and α_{2C} -ARs but also blocks 5-HT_{1A}, 5-HT_{2A}, 5-HT_{2C}, and histamine H₁ receptors.⁵

As part of our interest in the development of new α_2 -AR antagonists,^{6–10} we have previously described the synthesis and pharmacological evaluation of several series of diphenyl and phenyl substituted bis- and monoguanidine (e.g., 1 and 2, Figure 1) as well as bis- and mono-2-aminoimidazoline derivatives (e.g., 3, Figure 1), some of which have shown high affinity and antagonist activity at the α_2 -AR. Moreover, compounds 1 and 2, which increase levels of NA in vivo and

Received: October 23, 2014

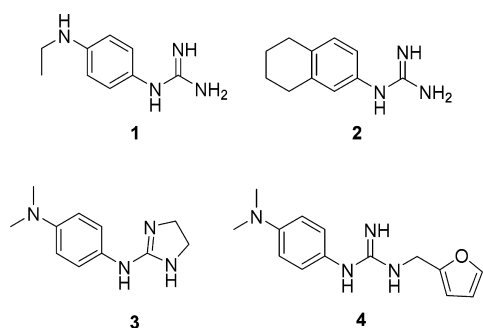


Figure 1. Structures of some high affinity α_2 -AR antagonists previously described in our group showing antidepressant activity (1 and 2), a 2-aminoimidazole (3), and a disubstituted guanidine (4).

present antidepressant properties in animal models,¹¹ have become our lead compounds.

Despite these good results, highly similar structures have often led to opposing functional activity at the receptor, with prediction of the features necessary for antagonist activity proving particularly difficult. However, we have recently described the design (by means of a pharmacophore), synthesis, and pharmacological evaluation of new phenyl-guanidinium and 2-aminoimidazolium derivatives with a second substitution in the guanidine moiety (e.g., 4, Figure 1). This added structural modification affords exclusively α_2 -AR antagonists (in contrast with the analogous monosubstituted compounds which had previously exhibited a mixture of antagonist/agonist activities) but has a detrimental effect on receptor affinity.¹²

Hence, we present in this article the synthesis of a series of guanidine and 2-aminoimidazole derivatives of pyridine as well as 1,4-dihydroquinazolin-2-amines (emanating from the promising pharmacological profiles of initial derivatives), the evaluation of their α_2 -AR binding affinity using *in vitro* assays in human PFC brain tissue, functional studies to determine the agonist or antagonist nature of a range of these molecules in human PFC brain tissue, and microdialysis experiments to assess the target engagement of our compounds *in vivo*. The primary aim of this work is to obtain compounds displaying solely antagonist activity at the α_2 -AR; thus, EC_{50} values against the known agonist UK14304 have also been measured providing several structure–activity relationships (SARs) related to both α_2 -AR affinity and activity.

RESULTS AND DISCUSSION

Design Strategy. As part of a ligand-based drug design strategy based on our previously developed pharmacophore, which contains two contiguous hydrophobic cores connected through a protonated N-containing fragment,¹² we propose to substitute one of the hydrophobic moieties by a pyridine as a bioisostere of the phenyl ring present in our previous derivatives.^{6–11} The introduction of a pyridine core will result in a number of beneficial characteristics. On the one hand, the pyridine ring is more metabolically stable because of its reduced lipophilicity relative to the phenyl ring.¹³ On the other hand, the high basicity of the phenylguanidine functionality (pK_{aH} of phenylguanidine is 10.88)¹⁴ will be substantially reduced (calculated pK_{aH} of 2-pyridinoguanidine is 9.54).¹⁵

Taking into account the mentioned basicity of these compounds, their conformation must be considered in terms of the guanidinium and 2-aminoimidazolium protonation

states existing under physiological conditions. Hence, we propose to synthesize molecules that can be considered as conformationally *controlled* analogues of our lead compounds 1–4 (Figure 1), allowing investigation of the importance of molecular conformation and rigidity on binding to, and antagonist activity at, the α_2 -AR. The pyridine ring and guanidinium/2-aminoimidazolium groups can adopt either a coplanar or out of plane arrangement relative to each other (Figure 2).

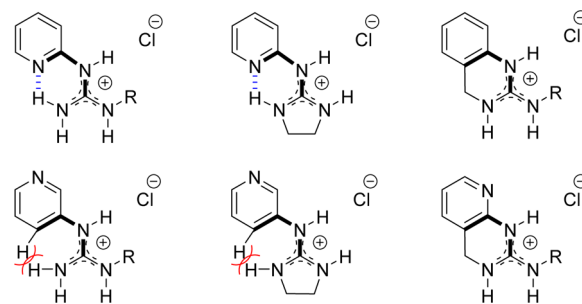
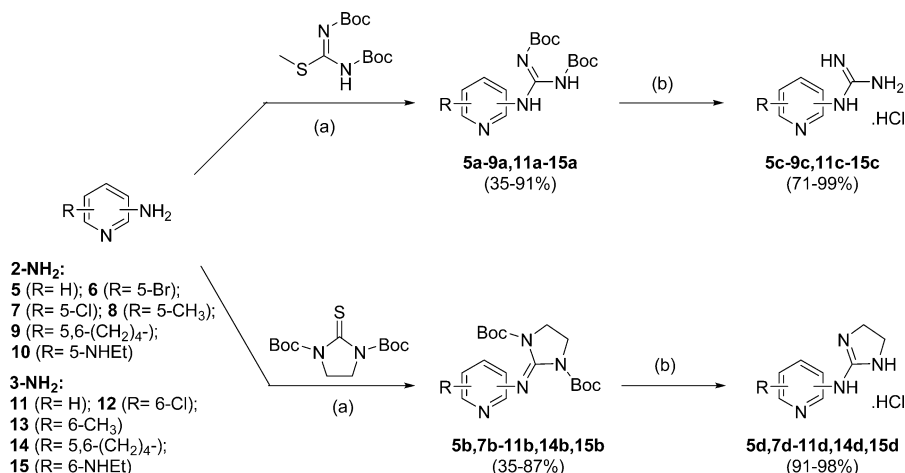


Figure 2. Conformational preferences of proposed compounds: pyridinylguanidines (left, up and down), 2-aminoimidazoles (middle, up and down), and constrained dihydroquinazoline/ dihydropyrido-pyrimidin-2-amines (right, up and down).

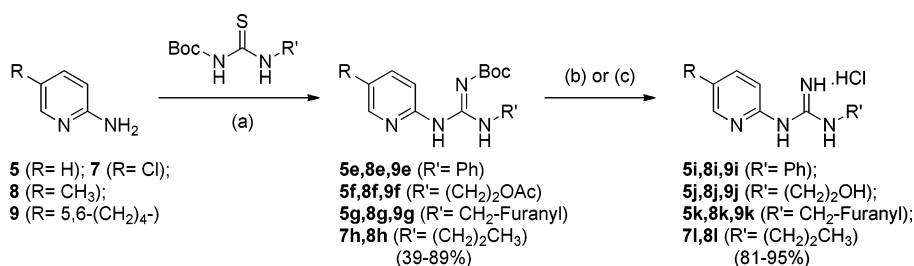
For pyridin-2-yl derivatives, an intramolecular hydrogen bond (IMHB) between the pyridine nitrogen lone-pair of electrons and a proton from either the guanidinium or 2-aminoimidazolium confers a coplanar arrangement. On the contrary, pyridin-3-yl derivatives are forced into an out of plane arrangement due to avoidance of repulsion between aromatic protons from the pyridine ring and NH protons from the cationic groups. We have previously examined these conformations in a theoretical and spectroscopic study and predicted that these preferences will be maintained in the aqueous environment of the body.¹⁶

Previous studies^{6–11} have instructed that substitution of the aryl ring para to the cationic group is favored for α_2 -AR affinity and activity and that steric bulk in that position is not well tolerated. Thus, the para-substituents found in lead compounds 1 (-NH₂) and 2 [-(CH₂)₄-] were prepared for all families (pyridin-2-yl and pyridin-3-yl; guanidines and 2-aminoimidazoles) because of their promising target engagement proved by microdialysis experiments^{6,7} and their pharmacological profiles as antidepressants in animal models.¹² Additionally, a series of substituents with diverse electronic effects were examined in an effort to obtain further SARs information.

Our previous pharmacophore¹² as well as the pharmacological results obtained from this new series of pyridinyl derivatives directed the choice of subsequent compounds to explore: substitution of the molecules beyond the cationic group (*N*-pyridinyl-*N'*-substituted guanidines) and further restraint of molecular conformation (1,4-dihydroquinazolin-2-amines). Furthermore, 1,4-dihydroquinazolin-2-amines and 1,4-dihydropyrido[2,3-*d*]pyrimidin-2-amines maintain many of the features of the first series of derivatives prepared while improving the pharmacokinetic profile of the compounds.¹⁷ However, it must also be stated that our arylguanidines have previously demonstrated an ability to cross the blood–brain barrier in animal models,^{6,7} probably via amino acid transporters.

Scheme 1. General Synthetic Scheme for the Preparation of Pyridino(guanidine/-2-aminoimidazoline) Hydrochlorides^a

^aReagents: (a) HgCl₂, NEt₃, CH₂Cl₂, rt; (b) HCl (4 M in 1,4-dioxane).

Scheme 2. General Synthetic Scheme for the Preparation of Disubstituted Guanidine Hydrochlorides^a

^aReagents: (a) HgCl₂, NEt₃, CH₂Cl₂, rt; (b) HCl (4 M in 1,4-dioxane); (c) HCl (4 M in methanol) for compounds **5f**, **8f**, and **9f**.

Chemistry. Boc-protected intermediates **5a–9a** and hydrochloride salts **5c–9c** (see Scheme 1) have been previously described by our group,¹⁶ while all remaining compounds are new, to the best of our knowledge, and none of the compounds have previously been tested for action at the α_2 -AR. The synthesis and characterization of all starting compounds and Boc-protected and neutral intermediates are presented in the Supporting Information. All compounds were tested pharmacologically as the hydrochloride salts because of their high water solubility.

Our standard synthetic approach for the guanidylation or 2-aminoimidazolidylation of poorly nucleophilic amines consists of the treatment of the corresponding starting amine with an activated *N*-Boc-protected thiourea¹⁸ or imidazolidine-2-thione¹⁹ in the presence of mercury(II) chloride and an excess of triethylamine to yield the corresponding Boc-protected intermediates, which can be converted to their hydrochloride salts on removal of the Boc group with hydrochloric acid solutions (Scheme 1).

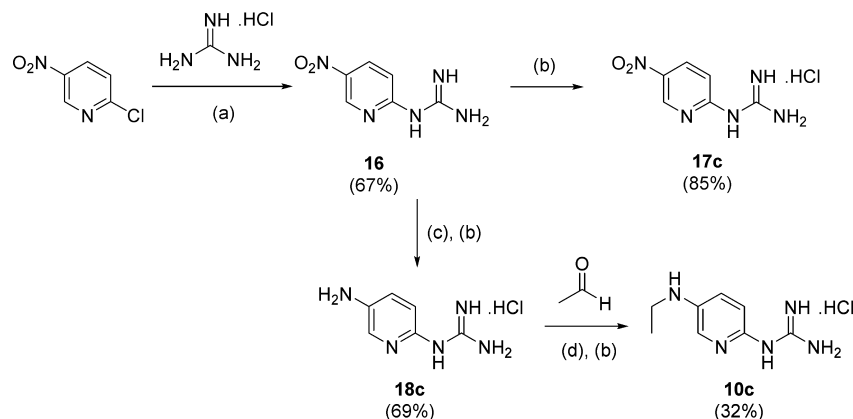
Accordingly, Boc-protected derivatives **5a–9a** and **11a–15a** were prepared from commercially available *N,N'*-di(*tert*-butoxycarbonyl)-*S*-methylisothiurea and compounds **5b**, **7b–11b**, **14b**, and **15b** from *N,N'*-di(*tert*-butoxycarbonyl)-imidazolidine-2-thione prepared from imidazolidine-2-thione (Scheme 1). Similarly, disubstituted Boc-protected guanidines **5e,f,g**, **7h**, **8e,f,g,h**, and **9e,f,g** were obtained from appropriate *N*-Boc-*N'*-substituted thioureas (Scheme 2).

All these Boc-protected intermediates were then deprotected using a solution of hydrochloric acid in dry 1,4-dioxane (4 M) to generate the corresponding hydrochloride salts **5c,d,i–k**, **6c**,

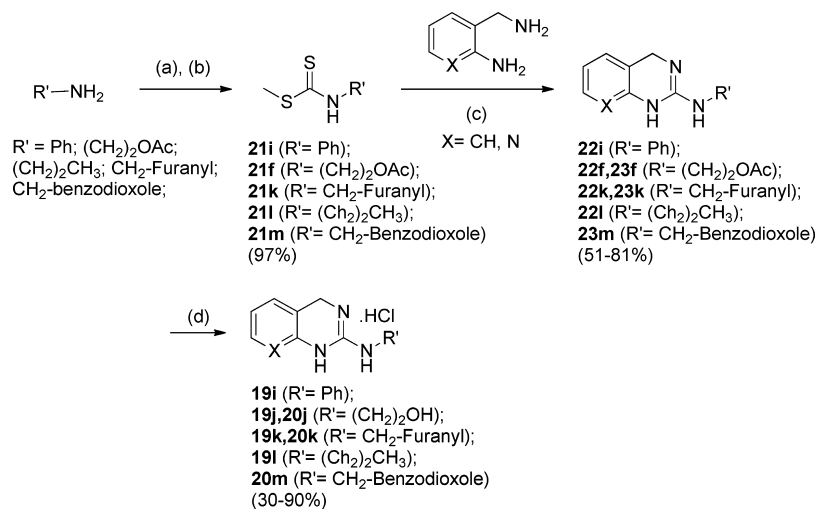
7c,d,l, **8c,d,i–l**, **9c,d,i–k**, **10c,d**, **11c,d**, **12c**, **13c**, **14c,d**, and **15d** (see Schemes 1 and 2) in good to excellent overall yields as presented in Table S1 (Supporting Information). These salts were purified by reverse phase silica C-8 chromatography, as well as recrystallization when required. Compounds **5e–g**, **7h**, **8e–h**, and **9e–g** were obtained as a mixture of two isomers as detected by NMR spectroscopy: the major product (*E*) in which the imine is in conjugation with the Boc group and the minor product (*Z*) in which the imine is in conjugation with the pyridine ring. The mixture of isomers was carried forward, as removal of the Boc group generated the same product regardless. This phenomenon has been extensively studied in our group computationally and by low temperature NMR.²⁰

It should be noted that compounds **5f**, **8f**, and **9f** show an acetate protection of the terminal OH group in the R' substituent; this was required to avoid formation of the cyclic 4,5-dihydrooxazole byproduct during mercury(II) chloride coupling. The acetate and Boc groups were simultaneously cleaved using methanolic hydrochloric acid solution to generate the corresponding guanidine hydrochlorides.

Because of problems with regioselectivity in the guanidylation of 2-amino-5-ethylaminopyridine, this methodology was unsuited to prepare compound **10c** and an alternative route was utilized. Nucleophilic aromatic substitution of 2-chloro-5-nitropyridine with the free base of guanidine hydrochloride (Scheme 3) proceeded smoothly yielding the neutral guanidine intermediate (**16**) that could be isolated after alkaline workup. This intermediate provided access to three hydrochloride salts: by treatment with HCl/1,4-dioxane, it yielded **17c**; palladium catalyzed hydrogenation followed by immediate protonation in

Scheme 3. Synthesis of Guanidine Hydrochlorides **10c**, **17c**, and **18c**^a

^aReagents: (a) NaOH, ^tBuOH, 82 °C, 8 h; (b) HCl (4 M in 1,4-dioxane); (c) H₂ (3 atm.), Pd/C (10%), CH₃OH; (d) NaBH(OAc)₃, CH₃CN/CH₃OH.

Scheme 4. Synthesis of Compounds **19i–l** and **20j,k,m** and Percentage Yields for Each Step^a

^aReagents: (a) CS₂, NEt₃, CH₂Cl₂, 0 °C, 15 min; (b) CH₃I, 0 °C to rt, 2 h; (c) K₂CO₃ (2.0 equiv), Cu(II)O (0.2 equiv), DMF, 60 °C, 2 h; (d) HCl (4 M in 1,4-dioxane or 1.25 M in CH₃OH).

HCl/1,4-dioxane gave **18c**; reductive alkylation with acetaldehyde and NaBH(OAc)₃ followed by protonation in HCl/1,4-dioxane afforded **10c**. The free-base compounds of the amino and *N*-ethylamino derivatives were unstable and needed to be converted to their corresponding hydrochloride salts in situ. All salts were purified by reverse-phase chromatography.

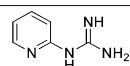
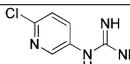
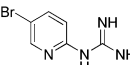
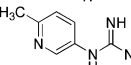
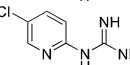
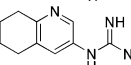
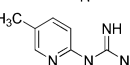
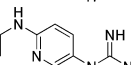
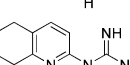
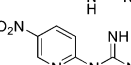
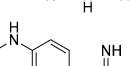
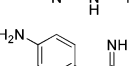
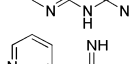
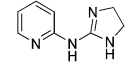
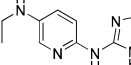
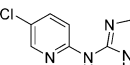
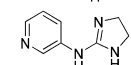
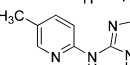
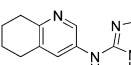
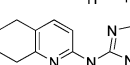
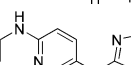
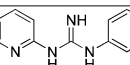
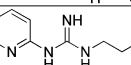
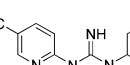
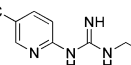
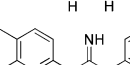
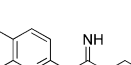
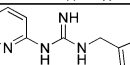
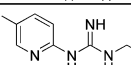
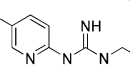
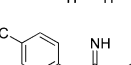
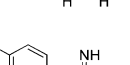
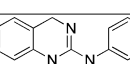
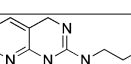
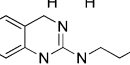
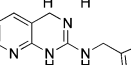
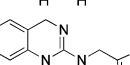
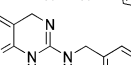
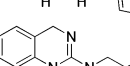
Informed by the pharmacological results from these initial sets of compounds, we proceeded to prepare two new series, the 2-amino-1,4-dihydroquinazoline and the 2-amino-1,4-dihydropyrido[2,3-*d*]pyrimidine derivatives **19i–l** and **20j,k,m**, which were synthesized using the method described by Das et al.²¹ This method involves the preparation of *S*-methyl-*N*-substituted dithiocarbamates from the corresponding amines, carbon disulfide, and iodomethane²² and coupling them with either 2-aminobenzylamine or 2-amino-3-aminopyridine in the presence of copper(II) oxide, followed by protonation in hydrochloric acid/1,4-dioxane (Scheme 4).

The yields obtained for the preparation of these derivatives are presented in Table S2 (Supporting Information). Similar to the disubstituted guanidine family, ethyl alcohol derivatives were protected as acetates to avoid formation of oxazolidin-2-thione. These intermediates were hydrolyzed in methanolic

hydrochloric acid (1.25 M), generating the desired hydrochloride salts (**19j** and **20j**).

Computational Physicochemical and Toxicity Parameters. Several physicochemical parameters such as molecular weight (MW), ClogP, ClogD (at pH 7.4), polar surface area (PSA), and pK_{aH}, which are associated with the absorption and distribution steps in the pharmacokinetic phase of a drug, were calculated using the Marvin package,¹⁵ and the results obtained are gathered in Table S3 (Supporting Information). According to different authors and different databases,²³ CNS-acting drugs already in the market show the following physicochemical characteristics: MW less than 400 with a mean value of 310 g mol⁻¹, (C)logP less than 5 with a preferred value around 1.5–2.7, 2.5, or 3.43 (depending on the authors), (C)logD greater than 0 and less than 3 (optimum value around 2.1), total PSA in the range 40–90 Å² and pK_{aH} between 7.5 and 10.5 (compounds that are positively charged at pH 7–8 favor brain penetration). The vast majority of our compounds fall within the desired ranges of these properties (see Table S3). These predicted values agree with our observations in animal studies that compounds administered peripherally and centrally led to increased levels of NA in rat brain (see microdialysis results and

Table 1. Affinity for the α_2 -AR (Expressed as pK_i) of All the Compounds Prepared^a

Compounds	pK_i	Compounds	pK_i
5c 	6.19 ± 0.08	12c 	5.18 ± 0.33
6c 	5.62 ± 0.07	13c 	4.97 ± 0.09
7c 	5.70 ± 0.19	14c 	5.57 ± 0.08
8c 	6.03 ± 0.09	15c 	6.35 ± 0.07
9c 	6.78 ± 0.08	17c 	5.00 ± 0.07
10c 	4.12 ± 0.06	18c 	5.00 ± 0.04
11c 	3.79 ± 0.20		
5d 	6.44 ± 0.08	10d 	5.65 ± 0.08
7d 	6.25 ± 0.07	11d 	5.28 ± 0.08
8d 	6.41 ± 0.13	14d 	7.02 ± 0.07
9d 	6.27 ± 0.09	15d 	7.13 ± 0.09
5i 	6.21 ± 0.07	5j 	5.38 ± 0.11
8i 	6.02 ± 0.09	8j 	5.21 ± 0.08
9i 	6.75 ± 0.06	9j 	5.83 ± 0.06
5k 	6.32 ± 0.04	7l 	5.71 ± 0.06
8k 	6.28 ± 0.05	8l 	6.74 ± 0.31
9k 	6.67 ± 0.06		
19i 	4.40 ± 0.11	20j 	4.49 ± 0.12
19j 	6.26 ± 0.08	20k 	4.50 ± 0.08
19k 	5.35 ± 0.07	20m 	5.30 ± 0.08
19l 	4.33 ± 0.06		

^aData represent the mean ± SEM of three to five separate experiments. The pK_i values of idazoxan and RX821002 (2-methoxyidazoxan) are 7.29 and 9.04, respectively.

ref 6). Taken together, it is reasonable to suggest that these compounds will have favorable pharmacokinetic profiles.

A very important cause of toxicity for many therapeutic agents is hERG channel blocking that results in cardiotoxicity and many drugs have been withdrawn from the market for that reason. Recently, a ligand-based pharmacophore for blocking hERG has been developed (and experimentally validated) using the Catalyst software;²⁴ in order to evaluate if our compounds fulfill such a pharmacophore, and hence produce cardiopathies, we have computationally optimized (DFT level: B3LYP/6-31+G*, PCM-water) four of them. These compounds (**8l**, **9c**, **9i** and **14d**) have been chosen as a sample of all the structures prepared.

The pharmacophoric elements identified in these four compounds as well as the distances among them compared to those of the Catalyst pharmacophore are gathered in Table S4 (Supporting Information). None of our compounds fulfill the pharmacophoric requirements, therefore, based on this model would not be able to block the hERG channels and, in principle, would have a lower probability to show cardiotoxicity.

Pharmacology and Structure–Activity Relationships.

Affinity for the α_2 -Adrenoceptors. The α_2 -AR affinity of all compounds was measured in human brain PFC tissue by competition assays with the selective radioligand [³H]-RX821002 (2-methoxyidazoxan), which was used at a constant concentration of 1 nM. The results obtained, expressed as pK_i values, are presented in Table 1.

On evaluation of the compounds binding affinity, it became clear that placement of the cationic group in the 2-position of the pyridine ring led to higher pK_i values (**5c–10c**, **17c–18c**, **5d**, **7d–10d**, **5i–k**, **8i–k**, **9i–k**, **7l–8l**, Table 1). For every *para*-substituent (R in Schemes 1 and 2), except for ethylamino, 2-guanidinopyridines had higher pK_i values than their 3-guanidinopyridine analogues (**11c–15c**). While this was also generally true for 2-aminoimidazolines (series d), the difference was less pronounced and pyridin-3-yl 2-aminoimidazolium compounds **14d** and **15d** gave the highest pK_i values of all. Comparing the differing cationic groups, it can be said that 2-aminoimidazoliums (series d) gave slightly higher pK_i values than the corresponding guanidiniums (series c), as has been seen for previous families of this type of compounds.

For derivatives with the cationic group at the 2-position of the pyridine ring, the most favorable aryl system was 5,6,7,8-tetrahydroquinoline (**9**), followed by unsubstituted pyridine (**5**) and then 5-methylpyridine (**8**). This trend is conserved for all guanidines (series c), 2-aminoimidazolines (series d) and disubstituted guanidines (series i, j, k and l). Pyridines with more inductively electron-withdrawing substituents, such as 5-Cl (**7**), -Br (**6**), -NO₂ (**17**) and -NH₂ (**18**), had poor affinity, while the 5-NHEt (**10**) substituted pyridines were the worst of all. On the contrary, the NHEt substituent gave the highest affinity molecules for pyridines with the cation at the 3-position of the pyridine ring (**15**) as shown in Table 1.

Extension into the region beyond the cationic moiety in disubstituted guanidines **5i,k**, and **8i,k,l**, led to higher values of binding affinity relative to analogous *mono*-substituted derivatives; however, this was not the case for compound **7l** which gave similar results to *mono*-substituted **7c**, and was the opposite for compounds **9i,j,k**, whose affinity was smaller or similar to the *mono*-substituted analogue (Table 1). The pK_i values varied with the group attached to the guanidine group, though the phenyl and 2-furanyl substituents (series i and k) consistently outperformed the ethanol substituent (series j).

Except for compound **19j**, 1,4-dihydroquinazoline and dihydropyridopyrimidin-2-amines systems (**19i,k,l** and **20j,k,m**) showed disappointingly low pK_i values at the α_2 -AR in this assay (Table 1). It is unclear why this is the case, though it could be due to the strain introduced to the system by the conformationally restricted six-membered ring. Maybe these restricted guanidines are too constrained and orient the substituents in the wrong direction; possibly a certain degree of flexibility, as that present in the hydrogen bonded 2-guanidinopyridines, is necessary for effective binding to the α_2 -AR. Curiously, in the 1,4-dihydroquinazoline series, the ethanol substituted compound (**19j**) had a considerably higher pK_i value than the phenyl (**19i**), 2-furanyl (**19k**), and *n*-propyl (**19l**) substituted systems, the reverse of that seen for disubstituted guanidines **5i–k**, **8i–k**, and **9i–k** (Table 1). This supports our hypothesis that the substituents in the conformationally restricted guanidines are in the wrong orientation.

[³⁵S]GTP γ S Binding Functional Assays. Compounds with a pK_i > 6.0, as well as some SAR-relevant compounds with lower pK_i values, were subjected to [³⁵S]GTP γ S functional experiments to determine their activity profile as agonist or antagonist of the α_2 -AR. As members of the GPCR superfamily, receptor activation leads to the exchange of GDP by GTP on the α -subunit. A direct evaluation of this G-protein activation can be made using radiolabeled GTP analogues. The [³⁵S]GTP γ S binding assay is a useful tool to distinguish between agonists (increasing the nucleotide binding), inverse agonists (decreasing the nucleotide binding), and neutral antagonists (not affecting the nucleotide binding) of GPCRs. The [³⁵S]GTP γ S nucleotide is not hydrolyzable, and hence once exchange occurs between GDP and [³⁵S]GTP γ S, the α -[³⁵S]GTP γ S subunit will not return to its GDP-bound state, meaning that activation of the receptor by ligands can be directly monitored using scintillation counting. Significantly, all compounds tested for activity (**5c–9c**, **12c**, **15c**, **5d**, **8d**, **9d**, **14d**, **15d**, **5i**, **9i**, **9j**, **5k**, **8k**, **9k**, **7l**, **8l**, **19j**) at the α_2 -AR proved to be either antagonists or inverse agonists, with no compounds activating the receptor. The corresponding dose–response curves for [³⁵S]GTP γ S binding versus ligand concentration can be found in Figure S1 (Supporting Information).

A subset of the compounds that did not stimulate receptor activation (**9c**, **9d**, **9k**, **14d**, **15d**, and **19j**) were tested in new [³⁵S]GTP γ S binding experiments against the known α_2 -AR agonist UK14304 to confirm that their inverse agonist/antagonist activity was mediated through α_2 -AR. In Table 2, the antagonist effect induced by the presence of a single concentration (10⁻⁵ M) of our compounds in the medium on UK14304 agonist stimulation of [³⁵S]GTP γ S binding can be found.

Addition of **9c**, **9d**, **14d**, and **15d** to the experiment induced a small (<10-fold) rightward shift in the EC₅₀ value for UK14304, suggesting that they possess only weak antagonistic effects at the α_2 -AR. On the contrary, **9k** and **19j** caused a substantial shift to the EC₅₀ of the standard agonist UK14304, characteristic of potent antagonists. The results obtained for **9k** and **19j**, which have slightly lower binding affinity than the monosubstituted guanidinium and 2-aminoimidazolium compounds tested, indicate improved α_2 -AR antagonistic features. It is reasonable to suggest that **9k** and **19j** have access to a pocket in the active site not available to **9c**, **9d**, **14d**, or **15d**, which allows them to block activation of the receptor by UK14304. The conformational restriction introduced in **19j**,

Table 2. EC₅₀ Values Obtained from the Concentration–Response Curves for UK14304 Stimulation of [³⁵S]GTPγS Binding (10⁻¹²–10⁻³ M, 10 Concentrations) in the Absence or Presence of the Different Compounds (10⁻⁵ M)

Experiment	EC ₅₀ (μM)
UK14304	0.906 ± 0.03
UK14304 + 9c	2.71 ± 0.27
UK14304 + 9d	3.57 ± 0.45
UK14304 + 9k	37.01 ± 4.71
UK14304 + 14d	4.23 ± 0.91
UK14304 + 15d	6.71 ± 0.58
UK14304 + 19j	60.34 ± 8.21

which may have induced a loss of receptor affinity, seems however to be ideal in order to orient the ethanol group in the proposed pocket and enhance antagonist activity.

In Vivo Microdialysis Experiments. It has been demonstrated that the administration of α₂-AR antagonists increases the in vivo release of NA in the PFC.²⁵ Considering their antagonistic effect and relatively good affinities over the α₂-ARs, **14d** and **15d** compounds were evaluated by microdialysis experiments. Local administration of **14d** by reverse dialysis through the probe (1–100 μM) induced a significant increase of extracellular NA levels in the PFC ($E_{\max} = 148 \pm 4\%$, $P < 0.001$; $F_{tr}[1,50] = 25.48$, $p < 0.0001$; $F_t[9,50] = 1.28$, $p = 0.26$; $F_i[9,50] = 4.70$, $p < 0.001$, $n = 7$; vs saline). When **15d** was perfused in the PFC an even larger increase of NA extracellular concentrations was observed ($E_{\max} = 429 \pm 7\%$, $P < 0.001$; $F_{tr}[1,50] = 182.7$, $p < 0.0001$; $F_t[9,50] = 45.97$, $p < 0.0001$; $F_i[9,50] = 54.64$, $p < 0.0001$, $n = 7$; vs saline). These results are presented in Figure 3.

Considering the positive results obtained by local administration of the compounds directly in the brain, we tested the

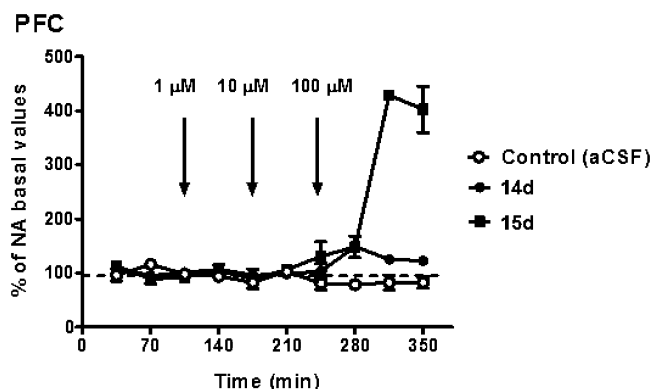


Figure 3. Effects of local administration of compounds **14d** and **15d** (1–100 μM) or aCSF in the PFC. Concentration of the compounds was progressively increased (arrows). Compounds were dissolved in aCSF and perfused via reverse dialysis at the time indicated by the arrows (every 70 min). Data correspond to the mean ± standard error mean values from three animals for each group and are expressed as percentages of the corresponding basal values.

effect of derivatives **14d** and **15d** on extracellular NA levels by systemic administration. Control rats were administered with the vehicle (saline), and intraperitoneal administration of compounds **14d** (10 mg/kg ip) and **15d** (10 mg/kg ip) significantly increased PFC NA extracellular concentration by $138 \pm 10\%$ ($F_{tr}[1,44] = 6.84$, $p < 0.05$; $F_t[10,44] = 2.47$, $p = 0.012$; $F_i[10,44] = 1.10$, $p = 0.38$, $n = 6$; vs saline) and $186 \pm 20\%$ ($F_{tr}[1,44] = 67.00$, $p < 0.0001$; $F_t[10,44] = 6.79$, $p < 0.0001$; $F_i[10,44] = 6.30$, $p < 0.0001$, $n = 6$; vs saline), respectively (see Figure 4).

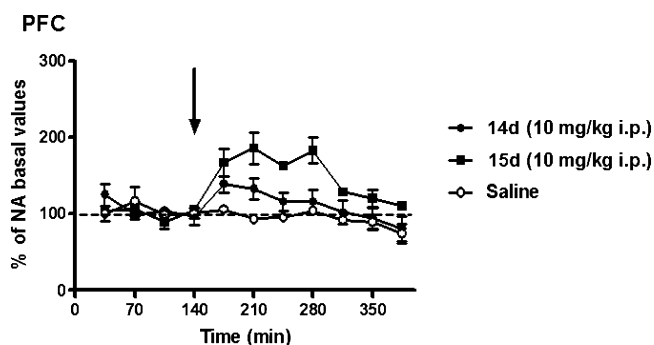


Figure 4. Effects of systemic **14d**, **15d**, or saline administration on extracellular NA concentrations evaluated in PFC. Data are mean ± SEM values from three to four experiments and are expressed as percentages of the corresponding basal values. The arrow represents administration of the different compounds or saline (1 mL kg⁻¹).

In summary, pyridine derivatives **14d** and **15d**, which are bioisosteric analogues of some of our previous phenyl derivatives that had been shown to be agonists,⁶ not only are α₂-AR antagonists in vivo but also keep that antagonistic activity when administered systemically, suggesting that they can cross the blood–brain barrier.

Structure–Activity Relationships and Docking Study.

A docking study was undertaken in order to understand the SAR observed in the α₂-AR competitive binding assays, keeping in mind that no crystal structure of any of the α₂-AR subtypes is known and that, therefore, the outcomes of this study could only be considered as hypotheses and guides for the design of future compounds. Hence, we used the Modeller 9.12 software²⁶ to construct homology models of the human α_{2A}-AR and α_{2C}-AR subtypes (the most prevalent subtypes in the human CNS²⁷) using sequences from www.uniprot.org (α_{2A}-AR, P08913; α_{2C}-AR, P18825), based on three template structures of the homologous β₂-adrenoceptor (β₂-AR; 2R4S,²⁸ 3D4S,²⁹ and 3SN6³⁰), which has 38.9% homology with the α_{2A}-AR and 35.2% homology with the α_{2C}-AR. Detailed information on the stepwise minimization process of homology model refinement carried out in explicit solvation using the AMBER software, binding site identification based on cocrystal structures of the β₂-adrenoceptor, and induced-fit docking in the MOE 2010 software can be found in the Supporting Information.

As expected, the smaller monosubstituted guanidines and 2-aminoimidazolines have lower docking scores (see Table S5, Supporting Information) than both disubstituted guanidines and 1,4-dihydroquinazolin-2-amines. Considering the molecular interactions and their boundaries as described by Stahl,³¹ we observed that these compounds could establish further interactions within the binding site, which is abundant in hydrophobic amino acids, favoring the binding of electron-rich

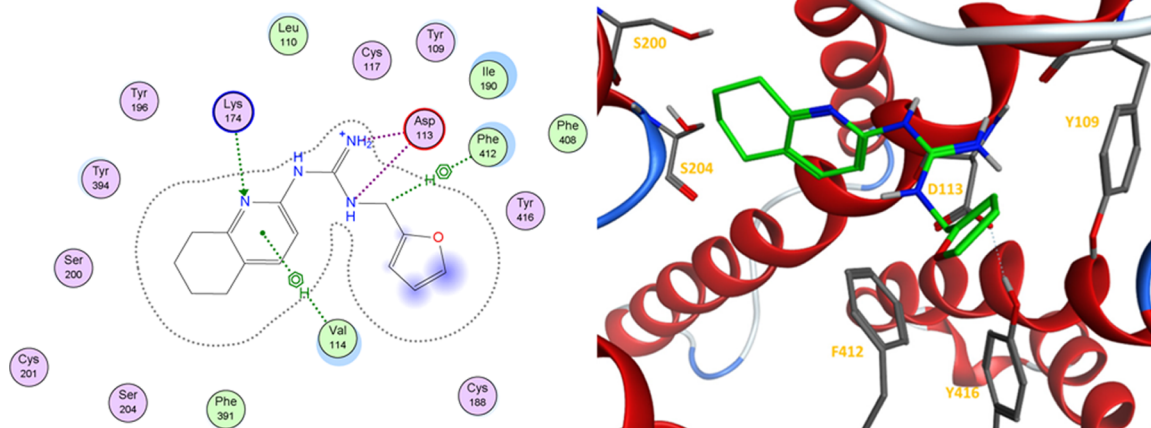


Figure 5. A 2D view of the interactions between **9k** and the α_{2A} -AR (left) and a 3D view from the extracellular side with important residues highlighted (right).

aryl systems. Strikingly, analysis of the top-ranked poses for all compounds revealed two main types of complex with both subtypes of the α_2 -AR.

First, the cationic group of monosubstituted derivatives generally interacts with Ser200 and Ser204 of the α_{2A} -AR (Ser214 and Ser218 of the α_{2C} -AR), the two residues implicated in catechol ligand-binding and receptor activation (cf. 3SN6 crystal structure of activated β_2 -AR). The only exceptions to this are 5,6,7,8-tetrahydroquinoline and ethylamino derivatives which preferentially fill the Ser200/Ser204 region of the receptor with their aryl core and orient the cationic group in proximity to Asp113 (Asp131 of the α_{2C} -AR), also heavily implicated in ligand binding.

Second, disubstituted guanidines and 1,4-dihydroquinazolines necessarily adopt a similar pose (Figure 5) in which the cationic group interacts with Asp113 of the α_{2A} -AR (Asp131 of the α_{2C} -AR), being unable to place the cationic group in the Ser200/Ser204 region. It was found that all such compounds bind in this manner and that furthermore the second substituent on the cationic moiety extends toward aromatic residues Tyr109, Phe412, and Tyr416 of TM-3 and TM-7 (Tyr127, Phe423, Tyr427 of the α_{2C} -AR). This helps to explain the enhanced and exclusive antagonist activity obtained for these compounds compared to monosubstituted derivatives, not only in the current series but also in analogous phenyl guanidine derivatives.

The exact docking scores are not instructive because of the inherent error associated with docking into homology models (scores are presented in Supporting Information Table S5); however, the information gained on the binding mode of compounds to the α_2 -AR and the implications this has on functional activity are highly valuable. Nonetheless, it is interesting that compounds **9i**, **9j**, and **9k** had the highest scores and are among the compounds with highest pK_i values. By comparison of docking into the α_{2A} -AR and α_{2C} -AR, the main ligand-binding residues described above are exactly homologous in both subtypes, and thus, the same types of pose are replicated. The main difference is in Tyr109 (α_{2A} -AR) or Tyr 127 (α_{2C} -AR), which is closer to ligands in the α_{2C} -AR because of a change in the position of extracellular loop 1 (ECL1) between TM-2 and TM-3. This leads to higher docking scores on average at the α_{2C} -AR; however, the trends among ligands are the same as in the α_{2A} -AR.

The pharmacophoric elements for binding of these compounds to the α_2 -AR can be summarized as follows: an aryl ring for hydrophobic interactions with the space of the receptor adjacent to Ser200/Ser204 (α_{2A} -AR) or Ser214/Ser218 (α_{2C} -AR), a cationic group for electrostatic binding to Asp113 (α_{2A} -AR) or Asp131 (α_{2C} -AR), and a substituent for hydrophobic interactions with the region formed by Tyr and Phe residues between TM-3 and TM-7. Therefore, the pharmacophore previously observed by us for α_2 -AR antagonists¹¹ has also been detected in these α_2 -AR docking experiments, which have provided extra information building on the previous pharmacophore. Thus, these α_2 -AR docking experiments have allowed us to see the residues in the region occupied by the second guanidinium substituent and have supported that “electron-rich aromatics” are suitable. The results also suggest that interaction with Ser200/Ser204 (Ser214/Ser218 of the α_{2C} -AR) should be circumvented in order to avoid receptor activation. This extra information can now be used to guide the design of new compounds.

Considering that the membrane preparation used in the experimental competitive binding assay is from human brain prefrontal cortex, a tissue rich in the α_{2C} -AR subtype, and given that compounds in our simulation seem to bind most favorably to the α_{2C} -AR model, it is possible that there could be a degree of subtype selectivity. It will be interesting to investigate this possibility, especially as there is a lack of α_{2C} -AR subtype-selective ligands. In this sense, the pharmacological modulation of the α_{2C} -AR subtype could contribute to attenuating some unwanted effects of adrenergic targeting drugs also mediated through α_{2A} -AR,³² and also, it has been hypothesized that α_{2C} -AR subtype antagonism may contribute to improve cognitive function.³³

CONCLUSIONS

In this paper we have reported the design, synthesis, and pharmacological evaluation of a series of 2- and 3-guanidino- and -2-aminoimidazolinopyridines, disubstituted 2-guanidino-pyridines, and N-substituted-2-amino-1,4-dihydroquinazolines with activity as antagonists of the α_2 -AR both in vitro and in vivo, with potential for the treatment of depression and schizophrenia.

All compounds have been prepared following different synthetic approaches developed in our laboratory. They have been evaluated for binding affinity and functional activity at the

α_2 -AR in human brain prefrontal cortex tissue, using competitive binding assays and [^{35}S]GTP γ S experiments, respectively. Furthermore, compounds with $pK_i > 7$ (**14d** and **15d**) were shown to increase NA levels in vivo by means of microdialysis experiments in rats, proving target engagement and showing antagonistic activity not only when they were locally administered but also when they were given systemically.

Several SARs, particularly in relation to binding affinity, have been obtained from a combination of our in vitro assays and computational docking models. Thus, it can be concluded that 2-guanidinopyridines have higher α_2 -AR affinity than analogous 3-guanidinopyridines; however, the opposite is the case for 2-aminoimidazolino derivatives. Generally speaking, 2-aminoimidazolino derivatives displayed higher α_2 -AR affinities than their monosubstituted guanidine analogues, as was expected from the results obtained in our previous work. In the present work, extension into the space beyond the cationic moiety, as in disubstituted guanidines, led to small increases in binding affinity, while such compounds are also conferred with enhanced antagonistic activity at the α_2 -AR as shown by their effects on UK14304 activation of the α_2 -AR.

Furthermore, for all arylguanidines and aryl-2-aminoimidazolines prepared exclusively, antagonist or inverse agonist activity was obtained, with no agonists found in [^{35}S]GTP γ S experiments. This work has identified six antagonists (**9c**, **9d**, **9k**, **14d**, **15d**, and **19j**) of the α_2 -AR which significantly reduce the ability of UK14304 to activate the receptor.

We have identified α_2 -AR antagonists that are water-soluble and exert their activity in vivo in rat brain with both central and peripheral administration. The potential for optimizing these compounds to obtain orally bioavailable agents that antagonize the α_2 -AR is huge, given the relevance of this receptor to the treatment of depression and schizophrenia.

■ EXPERIMENTAL SECTION

Pharmacology. [^3H]RX821002 Binding Assays. Specific [^3H]RX821002 binding was measured in 0.25 mL aliquots (50 mM Tris-HCl, pH 7.5) of the neural membranes, which were incubated in 96-well plates with [^3H]RX821002 (2 nM) for 30 min at 25 °C in the absence or presence of the competing compounds (10^{-12} – 10^{-3} M, 10 concentrations). Incubations were terminated by separating free ligand from bound ligand by rapid filtration under vacuum (1450 Filter Mate Harvester, PerkinElmer) through GF/C glass fiber filters. The filters were then rinsed three times with 300 μL of binding buffer, air-dried (60 min), and counted for radioactivity by liquid scintillation spectrometry using a MicroBeta TriLux counter (PerkinElmer). Specific binding was determined and plotted as a function of the compound concentration. Nonspecific binding was determined in the presence of adrenaline (10^{-5} M). Analyses of competition experiments to obtain the inhibition constant (K_i) were performed by nonlinear regression using the GraphPad Prism program. All experiments were analyzed assuming a one-site model of radioligand binding. K_i values were normalized to pK_i values

[^{35}S]GTP γ S Binding Assays. The incubation buffer for measuring [^{35}S]GTP γ S binding to brain membranes contained, in a total volume of 250 μL , 1 mM EGTA, 3 mM MgCl_2 , 100 mM NaCl, 50 mM GDP, 50 mM Tris-HCl at pH 7.4 and 0.5 nM [^{35}S]GTP γ S. Protein aliquots were thawed and resuspended in the same buffer. The incubation was started by addition of the membrane suspension (40 μg of membrane proteins) to the previous mixture and was performed at 30 °C for 120 min, with shaking. In order to evaluate the influence of the compounds on [^{35}S]GTP γ S binding, 10 concentrations (10^{-12} – 10^{-3} M) of the different compounds were added to the assay. Incubations were terminated by separating free ligand from bound ligand by rapid filtration under vacuum (1450 Filter Mate Harvester, PerkinElmer) through GF/C glass fiber filters. The filters were then rinsed three

times with 300 μL of incubation buffer and air-dried (60 min). The radioactivity trapped was determined by liquid scintillation spectrometry (MicroBeta TriLux counter, PerkinElmer). The [^{35}S]GTP γ S bound was about 7–14% of the total [^{35}S]GTP γ S added. Nonspecific binding of the radioligand was defined as the remaining [^{35}S]GTP γ S binding in the presence of 10 μM unlabeled GTP γ S. The pharmacological parameters of the stimulation curves of the [^{35}S]GTP γ S binding were obtained by nonlinear analysis using GraphPad Prism software version 5.0.

In Vivo Microdialysis Experiments. Animals. Experiments were performed on male Sprague–Dawley rats (University of the Basque Country, Spain). Animals were housed 4/5 per cage in a 12 h light–dark cycle at room temperature (22 °C) with food and water ad libitum. All the experimental protocols were approved by the Committee for Animal Experimentation at the University of the Basque Country (UPV/EHU). All procedures relating to animal care and use conformed to European Ethical Standards (6106/10-EEC) and Spanish Law (RD 53/2013).

Microdialysis Experiments. Male Sprague–Dawley rats (250–300 g) were implanted with a probe in a stereotaxic apparatus under 1.5% isoflurane anesthesia. The probe was located in the prefrontal cortex (PFC) according to the coordinates of the atlas of Paxinos and Watson³⁴ (AP (anterior to bregma), +2.8 mm; L (lateral from the mid-sagittal suture), +1 mm, DV (ventral from the dura surface), –5 mm).

Experiments were performed 18–24 h after the probe implantation, and artificial cerebrospinal fluid (aCSF: 148 mM NaCl, 2.7 mM KCl, 1.2 mM CaCl_2 , and 0.85 mM MgCl_2 ; pH 7.4) was pumped at a flow rate of 1 $\mu\text{L min}^{-1}$ (CMA/microdialysis infusion pump). Drugs, when locally administered, were dissolved in aCSF and applied during 70 min via dialysis probe in increasing concentrations of 1, 10, and 100 μM . Drugs systemically administered were dissolved in saline and injected intraperitoneally. In each experimental group, animals received either drugs or their appropriate vehicle.

Samples were collected every 35 min and NA concentrations analyzed by HPLC apparatus with amperometric detection (VT-03 cell, Decade II, Antec Leyden, Holland) at an oxidizing potential of 0.300 mV. The mobile phase (50 mM fosforic acid, 0.1 mM EDTA, 8 mM sodium chloride, 500 mg L^{-1} sodium octyl sulfate, pH 6, and 16% methanol) was filtered, degassed (Hewlett-Packard model 1100 degasser), and delivered at a flow rate of 0.2 mL/min by a Hewlett-Packard model 1100 pump. Stationary phase was a C18 column (ALF-205, 150 mm \times 2.1 mm, 3 μm ; Antec Leyden, Holland). Samples (injection volume 30 μL) were injected, and NA was analyzed in a run time of 18 min.

The mean values of the first three/four samples before drug administration were considered as 100% basal value. All measures of extracellular NA concentrations are expressed as percentage of the baseline value \pm SEM. Two-way analysis of variance (ANOVA) was followed by Bonferroni's test between control, and each treated group was assessed for statistical analysis. F values were expressed as $F_{t,r}$ (treatment, between groups), F_t (time, within groups), or F_i (treatment \times time, interaction). In these analyses all the experimental points, including basal values, were considered. All statistical procedures were performed using GraphPad Prism (GraphPad Software, San Diego, CA, USA).

At the end of the experiments, rats were killed by an overdose of anesthetic and the brains were dissected to check the correct implantation of the probe.

Chemistry. General. All commercial chemicals were obtained from either Sigma-Aldrich or Fluka and used without further purification. Deuterated solvents for NMR spectroscopy use were purchased from Apollo. Dry solvents were prepared using standard procedures, according to Vogel,³⁵ with distillation prior to use. Chromatographic columns were run using a Biotage SP4 flash purification system with Biotage SNAP silica cartridges. Solvents for synthesis purposes were used at GPR grade. Analytical TLC was performed using either Merck Kieselgel 60 F254 silica gel plates or Polygram Alox N/UV254 aluminum oxide plates. Visualization was by UV light (254 nm). NMR spectra were recorded on Bruker DPX-400

Avance spectrometers, operating at 400.13 and 600.1 MHz for ^1H NMR; 100.6 and 150.9 MHz for ^{13}C NMR. Shifts are referenced to the internal solvent signals.³⁶ NMR data were processed using Bruker TOPSPIN software. HRMS spectra were measured on a Micromass LCT electrospray TOF instrument with a WATERS 2690 autosampler and methanol/acetonitrile as carrier solvent. Melting points were determined using a Stuart Scientific melting point SMP1 apparatus and are uncorrected. Infrared spectra were recorded on a PerkinElmer Spectrum One FT-IR spectrometer equipped with a Universal ATR sampling accessory.

HPLC purity analysis was carried out using a Varian ProStar system equipped with a Varian Prostar 335 diode array detector and a manual injector (20 μL). For purity assessment, UV detection was performed at 245 nm, and peak purity was confirmed using a purity channel. The stationary phase consisted of an ACE 5 C18-AR column (150 mm \times 4.6 mm), and the mobile phase used the following gradient system, eluting at 1 mL/min: aqueous formate buffer (30 mM, pH 3.0) for 10 min, linear ramp to 85% methanol buffered with the same system over 25 min, hold at 85% buffered methanol for 10 min. Minimum requirement for purity was set at 95.0%.

Preparation of Hydrochloride Salts from Boc-Protected Derivatives: Procedure B. To either the 1-(pyridinyl)-2,3-di(*tert*-butoxycarbonyl)guanidine, 1-(pyridinyl)-2,3-di(*tert*-butoxycarbonyl)-2-iminoimidazolidine, or 1-(pyridinyl)-2-(*tert*-butoxycarbonyl)-3-substituted guanidine precursor (1.0 equiv, 0.5 mmol) were added 4 M HCl/1,4-dioxane (6.0 equiv per Boc group) and a 1:1 solution of $^t\text{PrOH}/\text{CH}_2\text{Cl}_2$, such as to maintain a reaction concentration of 0.2 M. The mixture was stirred at 55 $^\circ\text{C}$ until completion, as judged by disappearance of starting material in TLC. Solvent and excess HCl were then removed under vacuum, and the crude salt was dissolved in a minimum volume of water. It was washed with CH_2Cl_2 (2 \times 5 mL) and then purified using reverse phase chromatography (C-8 silica) with 100% H_2O as mobile phase. Removal of solvent yielded the pure guanidine/2-aminoimidazoline hydrochloride, which was recrystallized as described if deemed necessary.

General Procedure for the Protonation of Neutral Guanidines: Procedure D. To a solution of the corresponding neutral guanidine or N-substituted-1,4-dihydroquinazolin-2-amine (1.0 equiv, 0.5 mmol) in CH_2Cl_2 (0.5 mL) was added excess 4 M HCl/dioxane (3.0 equiv, 1.5 mmol, 375 μL). Where necessary CH_3OH (1 mL) was added dropwise as needed to aid solubility. Stirring was continued for 1 h after which solvent and excess HCl were removed under vacuum. The crude salt was then dissolved in a minimum volume of water, washed with CH_2Cl_2 (2 \times 5 mL), and purified using reverse phase chromatography (C-8 silica) with 100% H_2O as mobile phase. Where necessary, further purification was carried out.

1-(Pyridin-2-yl)guanidine Hydrochloride (5c): Procedure B. Colorless crystals (71%) after recrystallization from CH_3OH and Et_2O . Mp 77–78 $^\circ\text{C}$, clean melt. δ_{H} (600 MHz, $\text{DMSO}-d_6$): 7.07 (d, 1H, $J = 8.2$, Ar), 7.18 (dd, 1H, $J = 6.9$, 5.4, Ar), 7.88 (m, 1H, Ar), 8.30 (br s, 4H, NH), 8.32 (d, 1H, $J = 5.4$, Ar), 11.39 (br s, 1H, NH). δ_{C} (150 MHz, $\text{DMSO}-d_6$): 113.2 (CH Ar), 119.3 (CH Ar), 139.5 (CH Ar), 146.7 (CH Ar), 151.9 (q Ar), 155.3 (q, Gua). ν_{max} (ATR)/ cm^{-1} : 3312 (NH), 3180 (NH), 3130 (NH), 1679 (C=N), 1622, 1596, 1561, 1462, 1416, 1319, 1274, 1244, 1154, 1054, 1020, 998, 874, 775. HRMS (ESI^+) m/z : $[\text{M} + \text{H}]^+$ calcd for $\text{C}_6\text{H}_9\text{N}_4$ 137.0827. Found: 137.0827. Purity by HPLC: 97.2% ($t_{\text{R}} = 16.81$ min).

1-(Pyridin-2'-yl)-2-iminoimidazolidine Hydrochloride (5d): Procedure B. White solid (92%). Mp 155–160 $^\circ\text{C}$, decomposition. δ_{H} (600 MHz, $\text{DMSO}-d_6$): 3.73 (s, 4H, CH_2), 7.12 (d, 1H, $J = 8.4$, Ar), 7.20 (dd, 1H, $J = 7.0$, 5.3, Ar), 7.87 (dt, 1H, $J = 7.0$, 2.3, Ar), 8.33 (d, 1H, $J = 5.3$, Ar), 8.90 (br s, 2H, NH), 11.60 (br s, 1H, NH). δ_{C} (150 MHz, $\text{DMSO}-d_6$): 42.4 (2 CH_2), 112.7 (CH Ar), 119.6 (CH Ar), 139.4 (CH Ar), 147.1 (CH Ar), 150.7 (q Ar), 155.8 (q, Imi). ν_{max} (ATR)/ cm^{-1} : 3451, 3401, 3159 (NH), 3059 (NH), 2957, 2906, 2526, 2384, 2270, 1632 (C=N), 1594, 1476, 1448, 1426, 1366, 1344, 1279, 1247, 1199, 1158, 1102, 1053, 1017, 952, 932, 869, 772, 724, 693. HRMS (ESI^+) m/z : $[\text{M} + \text{H}]^+$ calcd for $\text{C}_8\text{H}_{11}\text{N}_4$ 163.0984. Found: 163.0979. Purity by HPLC: 97.2% ($t_{\text{R}} = 18.80$ min).

1-(Pyridin-2-yl)-3-(phenyl)guanidine Hydrochloride (5i): Procedure B. Colorless gum (90%). δ_{H} (400 MHz, $\text{DMSO}-d_6$): 7.19 (d, 1H, $J = 8.2$, Ar), 7.25 (dd, 1H, $J = 7.0$, 5.2, Ar), 7.40 (m, 3H, Ar), 7.53 (app t, 2H, $J = 8.1$, 7.4, Ar), 7.94 (app td, 1H, 7.0, 1.6, Ar), 8.38 (d, 1H, $J = 5.2$, Ar), 8.92 (br s, 2H, NH), 11.11 (br s, 1H, NH), 11.60 (br s, 1H, NH). δ_{C} (100 MHz, $\text{DMSO}-d_6$): 113.6 (CH Ar), 119.7 (CH Ar), 125.3 (CH Ar), 127.4 (CH Ar), 129.9 (CH Ar), 134.1 (q Ar), 139.8 (CH Ar), 146.6 (CH Ar), 151.9 (q Ar), 153.5 (q, CN). ν_{max} (ATR)/ cm^{-1} : 3061 (NH), 2953, 1668 (C=N), 1639, 1594, 1569, 1485, 1423, 1373, 1231, 1152, 1075, 779, 758, 696. HRMS (ESI^+) m/z : $[\text{M} + \text{H}]^+$ calcd for $\text{C}_{12}\text{H}_{13}\text{N}_4$ 213.1140. Found: 213.1145. Purity by HPLC: 97.6% ($t_{\text{R}} = 24.21$ min).

1-(Pyridin-2-yl)-3-(ethoxy)guanidine Hydrochloride (5j): Procedure B. White solid (83%). Mp 140–143 $^\circ\text{C}$, decomposition. δ_{H} (400 MHz, $\text{DMSO}-d_6$): 3.44 (t, 2H, $J = 5.2$, CH_2), 3.61 (t, 2H, $J = 5.2$, CH_2), 5.19 (br s, 1H, OH), 7.09 (d, 1H, $J = 8.3$, Ar), 7.18 (m, 1H, Ar), 7.88 (ddd, 1H, $J = 8.3$, 7.3, 1.1, Ar), 8.31 (dd, 1H, $J = 5.0$, 1.1, Ar), 8.56 (br s, 2H, NH), 9.65 (br s, 1H, NH), 11.33 (br s, 1H, NH). δ_{C} (100 MHz, $\text{DMSO}-d_6$): 44.1 (CH_2), 59.5 (CH_2), 113.6 (CH Ar), 119.5 (CH Ar), 140.0 (CH Ar), 146.8 (CH Ar), 152.8 (q Ar), 155.0 (q, CN). ν_{max} (ATR)/ cm^{-1} : 3449 (OH), 3026 (NH), 1600, 1518, 1492, 1445, 1406, 1358, 1278, 1250, 1185, 1107, 1040, 899, 873, 797, 754, 709, 683. HRMS (ESI^+) m/z : $[\text{M} + \text{H}]^+$ calcd for $\text{C}_9\text{H}_{13}\text{N}_4\text{O}$ 181.1089. Found: 181.1094. Purity by HPLC: 96.4% ($t_{\text{R}} = 18.11$ min).

1-(Pyridin-2-yl)-3-(2-furanyl)methyl)guanidine Hydrochloride (5k): Procedure B. White solid (82%). Mp 142–144 $^\circ\text{C}$, decomposition. δ_{H} (400 MHz, $\text{DMSO}-d_6$): 4.67 (d, 2H, $J = 5.0$, CH_2), 6.46–6.51 (m, 2H, Ar), 7.11 (d, 1H, $J = 8.2$, Ar), 7.21 (dd, 1H, $J = 6.9$, 5.2, Ar), 7.70 (dd, 1H, 1.6, 0.7, Ar), 7.90 (ddd, 1H, $J = 8.2$, 6.9, 1.3, Ar), 8.33 (dd, 1H, $J = 5.2$, 1.3, Ar), 8.86 (br s, 2H, NH), 9.71 (br s, 1H, NH), 11.32 (br s, 1H, NH). δ_{C} (100 MHz, $\text{DMSO}-d_6$): 38.2 (CH_2), 108.7 (CH Ar), 111.1 (CH Ar), 113.8 (CH Ar), 119.9 (CH Ar), 140.2 (CH Ar), 143.7 (CH Ar), 146.9 (CH Ar), 150.0 (q Ar), 152.5 (q Ar), 154.6 (q, CN). ν_{max} (ATR)/ cm^{-1} : 3092 (NH), 2990, 1674 (C=N), 1656, 1628, 1598, 1567, 1499, 1474, 1428, 1416, 1380, 1357, 1343, 1323, 1285, 1265, 1200, 1154, 1143, 1132, 1074, 1046, 1018, 997, 929, 915, 902, 875, 834, 784, 773, 748, 715. HRMS (ESI^+) m/z : $[\text{M} + \text{H}]^+$ calcd for $\text{C}_{11}\text{H}_{13}\text{N}_4\text{O}$ 217.1089. Found: 217.1090. Purity by HPLC: 95.5% ($t_{\text{R}} = 24.81$ min).

1-(5-Bromopyridin-2-yl) guanidine Hydrochloride (6c): Procedure B. White solid (74%). Mp 76–77 $^\circ\text{C}$, clean melt. δ_{H} (600 MHz, $\text{DMSO}-d_6$): 7.06 (d, 1H, $J = 8.8$, Ar), 8.09 (dd, 1H, $J = 8.8$, 2.5, Ar), 8.23 (br s, 4H, NH), 8.43 (d, 1H, $J = 2.5$, Ar), 11.53 (br s, 1H, NH). δ_{C} (150 MHz, $\text{DMSO}-d_6$): 114.7 (q Ar), 116.1 (CH, Ar), 142.9 (CH, Ar), 148.1 (CH, Ar), 151.7 (q, Ar), 155.9 (q, Gua). ν_{max} (ATR)/ cm^{-1} : 3313 (NH), 3218 (NH), 3011 (NH), 1684.0 (C=N), 1618, 1582, 1551, 1465, 1360, 1308, 1275, 1234, 1137, 1094, 1006, 925, 874, 825, 732. HRMS (ESI^+) m/z : $[\text{M} + \text{H}]^+$ calcd for $\text{C}_6\text{H}_8^{79}\text{BrN}_4$ 214.9932. Found: 214.9926. Purity by HPLC: 99.1% ($t_{\text{R}} = 23.88$ min).

1-(5-Chloropyridin-2-yl)guanidine Hydrochloride (7c): Procedure B. White solid (85%). Mp 162–164 $^\circ\text{C}$, clean melt. δ_{H} (600 MHz, $\text{DMSO}-d_6$): 7.13 (d, 1H, $J = 8.8$, Ar), 7.98 (dd, 1H, $J = 8.8$, 2.6, Ar), 8.28 (br s, 4H, NH), 8.35 (d, 1H, $J = 2.6$, Ar), 11.70 (br s, 1H, NH). δ_{C} (150 MHz, $\text{DMSO}-d_6$): 115.0 (CH Ar), 126.6 (q Ar), 139.2 (CH Ar), 144.7 (CH Ar), 151.0 (q Ar), 155.7 (q, Gua). ν_{max} (ATR)/ cm^{-1} : 3313 (NH), 3178 (NH), 2953, 1685 (C=N), 1617, 1587, 1551, 1465, 1364, 1310, 1274, 1236, 1136, 1113, 1022, 1009, 924, 876, 828, 757, 734, 718. HRMS (ESI^+) m/z : $[\text{M} + \text{H}]^+$ calcd for $\text{C}_6\text{H}_8^{35}\text{ClN}_4$ 171.0437. Found: 171.0433. Purity by HPLC: 99.0% ($t_{\text{R}} = 22.68$ min).

1-(5-Chloropyridin-2'-yl)-2-iminoimidazolidine Hydrochloride (7d): Procedure B. White solid (96%). Mp 95–96 $^\circ\text{C}$, clean melt. δ_{H} (600 MHz, $\text{DMSO}-d_6$): 3.70 (s, 4H, CH_2), 7.23 (d, 1H, $J = 8.8$, Ar), 7.96 (dd, 1H, $J = 8.8$, 2.7, Ar), 8.30 (d, 1H, $J = 2.7$, Ar), 8.86 (br s, 2H, NH), 12.31 (br s, 1H, NH). δ_{C} (150 MHz, $\text{DMSO}-d_6$): 42.5 (2 CH_2), 114.3 (CH Ar), 125.7 (q Ar), 139.1 (CH Ar), 145.2 (CH Ar), 149.5 (q Ar), 155.5 (q, Imi). ν_{max} (ATR)/ cm^{-1} : 3295, 3230 (NH), 3165 (NH), 3112 (NH), 3035, 2951, 1694, 1640 (C=N), 1628, 1588, 1569, 1501, 1468, 1442, 1389, 1365, 1301, 1276, 1231, 1180, 1137, 1111, 1047, 1017, 959, 930, 875, 832, 757, 687. HRMS

(ESI⁺) *m/z*: [M + H]⁺ calcd for C₈H₁₀N₄³⁵Cl 197.0594. Found: 197.0596. Purity by HPLC: 98.7% (*t_R* = 2.36 min).

1-(5-Chloropyridin-2-yl)-3-(propyl)guanidine Hydrochloride (7l): Procedure B. Yellow solid (93%). Mp 102–104 °C, clean melt. δ_{H} (600 MHz, DMSO-*d*₆): 0.94 (t, 3H, *J* = 7.4, CH₃), 1.59 (app sex, 2H, *J* = 7.4, 7.2, CH₂), 3.29 (m, 2H, CH₂), 7.12 (s, 1H, Ar), 7.99 (dd, 1H, *J* = 8.8, 2.5, Ar), 8.37 (d, 1H, *J* = 2.5, Ar), 8.58 (br s, 3H, NH), 9.17 (br s, 2H, NH), 11.47 (br s, 2H, NH). δ_{C} (150 MHz, DMSO-*d*₆): 11.3 (CH₃), 21.9 (CH₂), 42.9 (CH₂), 115.0 (CH Ar), 125.7 (q Ar), 139.7 (CH Ar), 145.1 (CH Ar), 151.0 (q Ar), 154.1 (q, CN). ν_{max} (ATR)/cm⁻¹: 3268 (NH), 3097 (NH), 3059, 2958, 2931, 2875, 1673, 1646 (C=N), 1629 (C=N), 1591, 1558, 1469, 1385, 1371, 1342, 1315, 1271, 1243, 1145, 1109, 1075, 1044, 1012, 966, 903, 869, 828, 772, 737, 658. HRMS (ESI⁺) *m/z*: [M + H]⁺ calcd for C₉H₁₂N₄³⁵Cl 211.0750. Found: 211.0745. Purity by HPLC: 99.3% (*t_R* = 26.40 min).

1-(5-Methylpyridin-2-yl)guanidine Hydrochloride (8c): Procedure B. Colorless crystals (84%) after recrystallization from ⁱPrOH and Et₂O. Mp 188–192 °C, clean melt. δ_{H} (600 MHz, DMSO-*d*₆): 2.27 (s, 3H, CH₃), 6.98 (d, 1H, *J* = 8.3, Ar), 7.71 (dd, 1H, *J* = 8.3, 1.9, Ar), 8.15 (d, 1H, *J* = 1.9, Ar), 8.21 (br s, 4H, NH), 11.17 (br s, 1H, NH). δ_{C} (150 MHz, DMSO-*d*₆): 17.1 (CH₃), 112.7 (CH Ar), 128.5 (q Ar), 140.1 (CH Ar), 146.1 (CH Ar), 149.7 (q Ar), 155.2 (q, Gua). ν_{max} (ATR)/cm⁻¹: 3268 (NH), 2889, 1677 (C=N), 1621, 1601, 1563, 1489, 1376, 1315, 1285, 1242, 1086, 1035, 1023, 1002, 909, 873, 832, 798, 738, 718. HRMS (ESI⁺) *m/z*: [M + H]⁺ calcd for C₇H₁₁N₄ 151.0984. Found: 151.0979. Purity by HPLC: 98.3% (*t_R* = 21.57 min).

1-(5-Methylpyridin-2-yl)-2-iminoimidazolidine Hydrochloride (8d): Procedure B. White solid (93%). Mp 140–145 °C, decomposition. δ_{H} (600 MHz, DMSO-*d*₆): 2.27 (s, 3H, CH₃), 3.71 (s, 4H, CH₂), 7.06 (d, 1H, *J* = 8.3, Ar), 7.70 (dd, 1H, *J* = 8.3, 2.0, Ar), 8.15 (d, 1H, *J* = 2.0, Ar), 8.84 (br s, 2H, NH), 11.76 (br s, 2H, NH). δ_{C} (150 MHz, DMSO-*d*₆): 17.2 (CH₃), 42.4 (2 CH₂), 112.3 (CH Ar), 128.7 (q Ar), 139.9 (CH Ar), 146.6 (CH Ar), 148.6 (q Ar), 155.8 (q, Imi). ν_{max} (ATR)/cm⁻¹: 3287 (NH), 3123 (NH), 2909, 2702, 2473, 2373, 2073, 1642 (C=N), 1599, 1578, 1486, 1454, 1373, 1297, 1280, 1257, 1238, 1222, 1141, 1077, 1032, 989, 935, 918, 875, 860, 831, 790, 741, 721. HRMS (ESI⁺) *m/z*: [M + H]⁺ calcd for C₉H₁₃N₄ 177.1140. Found: 177.1145. Purity by HPLC: 96.4% (*t_R* = 22.31 min).

1-(5-Methylpyridin-2-yl)-3-(phenyl)guanidine Hydrochloride (8i): Procedure B. Colorless gum (86%). δ_{H} (400 MHz, DMSO-*d*₆): 2.30 (s, 3H, CH₃), 7.10 (d, 1H, *J* = 8.4, Ar), 7.37–7.41 (m, 3H, Ar), 7.52 (app t, 2H, *J* = 8.0, 7.5, Ar), 7.78 (dd, 1H, *J* = 8.4, 1.8, Ar), 8.21 (d, 1H, *J* = 1.8, Ar), 8.93 (br s, 2H, NH), 11.43 (br s, 2H, NH). δ_{C} (100 MHz, DMSO-*d*₆): 17.7 (CH₃), 113.7 (CH Ar), 125.6 (CH Ar), 127.7 (CH Ar), 129.3 (q Ar), 130.3 (CH Ar), 134.8 (q Ar), 140.9 (CH Ar), 146.4 (CH Ar), 150.3 (q Ar), 153.9 (q, CN). ν_{max} (ATR)/cm⁻¹: 2921, 1637 (C=N), 1608, 1595, 1572, 1483, 1369, 1281, 1233, 1140, 1029, 900, 895, 827, 752. HRMS (ESI⁺) *m/z*: [M + H]⁺ calcd for C₁₃H₁₅N₄ 227.1297. Found: 227.1297. Purity by HPLC: 98.9% (*t_R* = 27.09 min).

1-(5-Methylpyridin-2-yl)-3-(ethoxy)guanidine Hydrochloride (8j): Procedure B. White solid (87%). Mp 150–154 °C, decomposition. δ_{H} (400 MHz, DMSO-*d*₆): 2.27 (s, 3H, CH₃), 3.42 (t, 2H, *J* = 5.0, CH₂), 3.60 (t, 2H, *J* = 5.0, CH₂), 5.20 (br s, 1H, OH), 7.01 (d, 1H, *J* = 8.3, Ar), 7.72 (dd, 1H, *J* = 8.3, 2.0, Ar), 8.14 (d, 1H, *J* = 2.0, Ar), 8.53 (br s, 2H, NH), 9.59 (br s, 1H, NH), 11.41 (br s, 1H, NH). δ_{C} (100 MHz, DMSO-*d*₆): 17.7 (CH₃), 44.1 (CH₂), 59.5 (CH₂), 113.1 (CH Ar), 128.7 (q Ar), 140.7 (CH Ar), 146.2 (CH Ar), 150.6 (q Ar), 154.9 (q, CN). ν_{max} (ATR)/cm⁻¹: 3352 (OH), 3234 (OH), 3169 (NH), 3001 (NH), 2917, 1670 (C=N), 1652, 1633, 1608, 1492, 1459, 1380, 1354, 1312, 1278, 1246, 1200, 1183, 1150, 1084, 1027, 996, 923, 887, 818, 762, 732, 718, 665. HRMS (ESI⁺) *m/z*: [M + H]⁺ calcd for C₉H₁₅N₄O 195.1246. Found: 195.1245. Purity by HPLC: 98.2% (*t_R* = 21.83 min).

1-(5-Methylpyridin-2-yl)-3-(2-furanylmethyl)guanidine Hydrochloride (8k): Procedure B. White solid (95%). Mp 130–135 °C, clean melt. δ_{H} (400 MHz, DMSO-*d*₆): 2.27 (s, 3H, CH₃), 4.66 (s, 2H, CH₂), 6.46–6.49 (m, 2H, Ar), 7.02 (d, 1H, *J* = 8.3, Ar), 7.69 (d, 1H, *J* = 0.6, Ar), 7.73 (dd, 1H, *J* = 8.3, 2.0, Ar), 8.15 (d, 1H, *J* = 2.0, Ar), 8.81 (br s, 2H, NH), 9.66 (br s, 1H, NH), 11.35 (br s, 1H, NH).

δ_{C} (100 MHz, DMSO-*d*₆): 17.7 (CH₃), 38.2 (CH₂), 108.7 (CH Ar), 111.1 (CH Ar), 113.4 (CH Ar), 129.0 (q Ar), 140.8 (CH Ar), 143.6 (CH Ar), 146.2 (CH Ar), 150.0 (q Ar), 150.5 (q Ar), 154.6 (q, CN). ν_{max} (ATR)/cm⁻¹: 3102 (NH), 1664 (C=N), 1623, 1609, 1493, 1407, 1381, 1355, 1274, 1247, 1225, 1210, 1158, 1083, 1077, 1018, 925, 912, 882, 821, 771, 748, 669. HRMS (ESI⁺) *m/z*: [M + H]⁺ calcd for C₁₂H₁₅N₄O 231.1246. Found: 231.1241. Purity by HPLC: 98.4% (*t_R* = 26.96 min).

1-(5-Methylpyridin-2-yl)-3-(propyl)guanidine Hydrochloride (8l): Procedure B. Yellow solid (90%). Mp 100–102 °C, clean melt. δ_{H} (600 MHz, DMSO-*d*₆): 0.94 (t, 3H, *J* = 7.5, CH₃), 1.58 (app sex, 2H, *J* = 7.5, 7.1, CH₂), 2.25 (s, 3H, CH₃), 3.29 (m, 2H, CH₂), 6.99 (br s, 1H, Ar), 7.71 (dd, 1H, *J* = 8.4, 1.9, Ar), 8.14 (d, 1H, *J* = 1.9, Ar), 8.59 (br s, 3H, NH), 9.43 (br s, 2H, NH), 11.34 (br s, 2H, NH). δ_{C} (150 MHz, DMSO-*d*₆): 11.0 (CH₃), 17.2 (CH₃), 21.6 (CH₂), 42.5 (CH₂), 112.6 (CH Ar), 128.3 (q Ar), 140.3 (CH Ar), 145.8 (CH Ar), 150.0 (q Ar), 154.1 (q, CN). ν_{max} (ATR)/cm⁻¹: 2965, 1674 (C=N), 1632, 1608, 1572, 1484, 1343, 1283, 1244, 1136, 1079, 1029, 968, 831, 743. HRMS (ESI⁺) *m/z*: [M + H]⁺ calcd for C₁₀H₁₇N₄ 193.1453. Found: 193.1461. Purity by HPLC: 96.9% (*t_R* = 24.57 min).

1-(5,6,7,8-Tetrahydroquinolin-2-yl)guanidine Hydrochloride (9c): Procedure B. Colorless crystals (87%) after recrystallization from CH₃OH and Et₂O. Mp 224–228 °C, decomposition. δ_{H} (600 MHz, DMSO-*d*₆): 1.73 (m, 2H, CH₂), 1.80 (m, 2H, CH₂), 2.68 (app t, 2H, *J* = 6.1, 6.0, CH₂), 2.78 (app t, 2H, *J* = 6.1, 6.0, CH₂), 6.80 (d, 1H, *J* = 8.2, Ar), 7.55 (d, 1H, *J* = 8.2, Ar), 8.22 (br s, 4H, NH), 11.08 (br s, 1H, NH). δ_{C} (150 MHz, DMSO-*d*₆): 22.1 (CH₂), 22.2 (CH₂), 27.2 (CH₂), 31.5 (CH₂), 110.5 (CH Ar), 127.3 (q Ar), 140.1 (CH Ar), 149.2 (q Ar), 154.0 (q Ar), 155.2 (q, Gua). ν_{max} (ATR)/cm⁻¹: 3323 (NH), 3149 (NH), 2961, 1679 (C=N), 1634, 1597, 1566, 1465, 1031, 813. HRMS (ESI⁺) *m/z*: [M + H]⁺ calcd for C₁₀H₁₅N₄ 191.1297. Found: 191.1293. Purity by HPLC: 98.1% (*t_R* = 27.00 min).

1-(5,6,7,8-Tetrahydroquinolin-2-yl)-2-iminoimidazolidine Hydrochloride (9d): Procedure B. White solid (93%). Mp 208–212 °C, decomposition. δ_{H} (600 MHz, DMSO-*d*₆): 1.72–1.76 (m, 2H, CH₂), 1.79–1.83 (m, 2H, CH₂), 2.69 (app t, 2H, *J* = 5.9, 6.3, CH₂), 2.84 (app t, 2H, *J* = 6.1, 6.4, CH₂), 3.73 (s, 4H, CH₂), 6.92 (d, 1H, *J* = 8.2, Ar), 7.54 (d, 1H, *J* = 8.2, Ar), 8.79 (br s, 2H, NH), 11.87 (br s, 1H, NH). δ_{C} (150 MHz, DMSO-*d*₆): 22.2 (CH₂), 22.2 (CH₂), 27.3 (CH₂), 31.5 (CH₂), 42.5 (2 CH₂), 110.1 (CH Ar), 127.5 (q Ar), 139.9 (CH Ar), 148.1 (q Ar), 154.8 (q Ar), 155.9 (q, Imi). ν_{max} (ATR)/cm⁻¹: 3344, 3296, 3169 (NH), 3114 (NH), 3058 (NH), 2934, 2848, 1642 (C=N), 1595, 1583, 1474, 1464, 1415, 1377, 1351, 1309, 1286, 1264, 1204, 1156, 1137, 1111, 1089, 1066, 1018, 949, 938, 927, 896, 864, 835, 817, 759, 736. HRMS (ESI⁺) *m/z*: [M + H]⁺ calcd for C₁₂H₁₇N₄ 217.1453. Found: 217.1458. Purity by HPLC: 97.0% (*t_R* = 26.65 min).

1-(5,6,7,8-Tetrahydroquinolin-2-yl)-3-(phenyl)guanidine Hydrochloride (9i): Procedure B. White solid (86%). Mp 180–183 °C, decomposed. δ_{H} (600 MHz, DMSO-*d*₆): 1.75 (app t, 2H, *J* = 5.6, 5.1, CH₂), 1.81 (app t, 2H, *J* = 5.8, 5.1, CH₂), 2.71 (app t, 2H, *J* = 5.6, CH₂), 2.79 (d, 2H, *J* = 5.8, CH₂), 6.92 (d, 1H, *J* = 8.2, Ar), 7.35 (t, 1H, *J* = 7.3, Ar), 7.39 (d, 2H, *J* = 7.6, Ar), 7.50 (app t, 2H, *J* = 7.6, 7.3, Ar), 7.60 (d, 1H, *J* = 8.2, Ar), 9.03 (br s, 2H, NH), 11.40 (br s, 1H, NH), 11.63 (br s, 1H, NH). δ_{C} (150 MHz, DMSO-*d*₆): 22.4 (CH₂), 22.5 (CH₂), 27.5 (CH₂), 31.8 (CH₂), 111.6 (CH Ar), 124.8 (CH Ar), 127.1 (CH Ar), 127.7 (q Ar), 130.1 (CH Ar), 140.6 (CH Ar), 135.3 (q Ar), 150.3 (q Ar), 153.6 (q Ar), 154.0 (q, CN). ν_{max} (ATR)/cm⁻¹: 3235 (NH), 2978, 2937, 1672, 1642 (C=N), 1595, 1578, 1499, 1467, 1376, 1319, 1282, 1234, 1121, 1079, 1047, 951, 835, 818, 755, 697, 664. HRMS (ESI⁺) *m/z*: [M + H]⁺ calcd for C₁₆H₁₉N₄ 267.1610. Found: 267.1605. Purity by HPLC: 95.6% (*t_R* = 31.11 min).

1-(5,6,7,8-Tetrahydroquinolin-2-yl)-3-(ethoxy)guanidine Hydrochloride (9j): Procedure B. White solid (81%). Mp 74–76 °C, clean melt. δ_{H} (400 MHz, DMSO-*d*₆): 1.70–1.82 (m, 4H, 2 CH₂), 2.67 (app t, 2H, *J* = 6.3, 5.9, CH₂), 2.76 (app t, 2H, *J* = 6.3, 6.0, CH₂), 3.43 (app t, 2H, *J* = 5.2, 4.9, CH₂), 3.61 (app t, 2H, *J* = 5.2, 4.9, CH₂), 5.21 (br s, 1H, OH), 6.82 (d, 1H, *J* = 8.2, Ar), 7.54 (d, 1H, *J* = 8.2, Ar), 8.45 (br s, 2H, NH), 10.10 (br s, 1H, NH), 11.15 (br s, 1H, NH). δ_{C} (100 MHz, DMSO-*d*₆): 22.6 (CH₂), 22.6 (CH₂), 27.6 (CH₂), 31.9

(CH₂), 44.1 (CH₂), 59.4 (CH₂), 110.7 (CH Ar), 127.5 (q Ar), 140.6 (CH Ar), 150.0 (q Ar), 154.0 (q Ar), 154.9 (q, CN). ν_{\max} (ATR)/cm⁻¹: 3405 (OH), 3317 (OH), 2937, 1673 (C=N), 1593, 1646, 1493, 1253, 1052, 815, 749. HRMS (ESI⁺) m/z : [M + H]⁺ calcd for C₁₂H₁₉N₄O 235.1559. Found: 235.1559. Purity by HPLC: 96.4% (t_R = 26.89 min).

1-(5,6,7,8-Tetrahydroquinolin-2-yl)-3-(2-furanylmethyl)guanidine Hydrochloride (9k): Procedure B. White solid (86%) was obtained as a white solid. Mp 182–186 °C, decomposition. δ_H (400 MHz, DMSO-*d*₆): 1.69–1.82 (m, 4H, 2 CH₂), 2.67 (app t, 2H, J = 6.0, 5.8, CH₂), 2.73 (app t, 2H, J = 6.3, 5.8, CH₂), 4.66 (s, 2H, CH₂), 6.46–6.49 (m, 1H, Ar), 6.50 (d, 1H, J = 2.8, Ar), 6.84 (d, 1H, J = 8.2, Ar), 7.55 (d, 1H, J = 8.2, Ar), 7.69 (s, 1H, Ar), 8.87 (br s, 2H, NH), 9.97 (br s, 1H, NH), 11.22 (br s, 1H, NH). δ_C (100 MHz, DMSO-*d*₆): 22.5 (CH₂), 22.6 (CH₂), 27.6 (CH₂), 31.8 (CH₂), 38.3 (CH₂), 108.7 (CH Ar), 111.0 (CH Ar), 111.1 (CH Ar), 127.8 (q Ar), 140.74 (CH Ar), 143.7 (CH Ar), 149.9 (q Ar), 150.0 (q Ar), 154.0 (q Ar), 154.6 (q, CN). ν_{\max} (ATR)/cm⁻¹: 3150 (NH), 2938, 1643 (C=N), 1603, 1472, 1281, 1179, 1062, 1012, 802, 734. HRMS (ESI⁺) m/z : [M + H]⁺ calcd for C₁₅H₁₉N₄O 271.1559. Found: 271.1563. Purity by HPLC: 98.4% (t_R = 30.64 min).

1-[5-(Ethylamino)pyridin-2-yl]guanidine Hydrochloride (10c). To a solution of neutral 1-(5-aminopyridin-2-yl)guanidine (111 mg, 0.73 mmol) in a mixture of CH₃CN/CH₃OH (5:1, 3.0 mL) was added acetaldehyde (1.0 equiv, 0.73 mmol, 41 μ L). The solution was stirred under an argon atmosphere, and sodium triacetoxyborohydride (2.0 equiv, 311 mg, 1.47 mmol) was added. Reaction was continued for 6 h, after which excess solvent and acetaldehyde were removed under reduced pressure. The resulting residue was dissolved in a solution of *i*PrOH/CH₂Cl₂ (20%, 10 mL), washed with NaHCO₃ (sat., 5 mL) and water (3 mL), dried over MgSO₄, filtered, and concentrated under vacuum. The residue was stirred in a 1.25 M methanolic HCl solution (4.0 equiv, 2.4 mL, 2.94 mmol) for 3 h. Excess solvent and HCl were removed under reduced pressure, and the residue was dissolved in a minimum volume of H₂O. The aqueous layer was washed with CH₂Cl₂ and concentrated under vacuum to yield a red solid, which was purified by reverse phase chromatography (C-8 silica) with 100% H₂O as mobile phase to yield a dark red solid identified by ¹H NMR spectroscopy as a mixture of salts. Normal phase chromatography, eluting with a gradient of CH₂Cl₂/CMA, isolated neutral guanidine (32%) as a red solid after restirring in 1.25 M methanolic HCl (2.4 mL). Mp 154–157 °C, clean melt. δ_H (400 MHz, DMSO-*d*₆): 1.22 (t, 3H, J = 7.2, CH₃), 3.43 (q, 2H, J = 7.2, CH₂), 7.12 (d, 1H, J = 9.4, Ar), 7.66 (br s, 4H, NH), 7.75 (d, 1H, J = 9.4, Ar), 7.92 (s, 1H, Ar), 9.78 (br s, 1H, NH). δ_C (100 MHz, DMSO-*d*₆): 13.7 (CH₃), 37.0 (CH₂), 114.3 (CH Ar), 120.7 (q Ar), 135.0 (CH Ar), 142.0 (CH Ar), 142.0 (q Ar), 157.2 (q, Gua). ν_{\max} (ATR)/cm⁻¹: 3313, 3181 (NH), 3130 (NH), 3037 (NH), 2973, 2810, 1702, 1666 (C=N), 1608, 1584, 1498, 1469, 1456, 1432, 1337, 1302, 1272, 1230, 1183, 1123, 1102, 1057, 1037, 1003, 942, 909, 875, 857, 821, 781, 730, 694, 672. HRMS (ESI⁺) m/z : [M + H]⁺ calcd for C₈H₁₄N₅ 180.1249. Found: 180.1244. Purity by HPLC: 99.5% (t_R = 3.88 min).

1-[5-(Ethylamino)pyridin-2'-yl]2-iminoimidazolidine Hydrochloride (10d): Procedure B. Colorless solid (93%). Mp above 220 °C, decomposition. δ_H (400 MHz, DMSO-*d*₆): 1.22 (m, 3H, CH₃), 3.44 (m, 2H, CH₂), 3.64 (s, 4H, CH₂), 7.16 (d, 1H, J = 8.0, Ar), 7.77 (d, 1H, J = 8.0, Ar), 7.91 (s, 1H, Ar), 8.58 (br s, 2H, NH), 9.32 (s, 1H, NH, NHet), 10.65 (br s, 1H, NH). δ_C (100 MHz, DMSO-*d*₆): 14.1 (CH₃), 37.6 (CH₂), 43.2 (2 CH₂), 114.6 (CH Ar), 122.0 (q Ar), 134.1 (CH Ar), 141.6 (CH Ar), 152.2 (q Ar), 159.4 (q, Imi). ν_{\max} (ATR)/cm⁻¹: 3375 (NH), 3198 (NH), 3057 (NH), 2860, 1675, 1619 (C=N), 1590, 1482, 1458, 1407, 1375, 1321, 1280, 1213, 1154, 1128, 1110, 1085, 1003, 938, 935, 785, 746, 717, 658. HRMS (ESI⁺) m/z : [M + H]⁺ calcd for C₁₀H₁₆N₅ 206.1406. Found: 206.1401. Purity by HPLC: 100.0% (t_R = 5.07 min).

1-(Pyridin-3-yl)guanidine Hydrochloride (11c): Procedure B. White solid (85%). Mp 65–67 °C, clean melt. δ_H (600 MHz, DMSO-*d*₆): 7.70 (m, 1H, Ar), 7.80 (br s, 4H, NH), 7.95 (d, 1H, J = 7.8, Ar), 8.62 (s, 1H, Ar), 8.68 (s, 1H, Ar), 10.33 (br s, 1H, NH). δ_C (150 MHz, DMSO-*d*₆): 125.5 (CH Ar), 133.6 (q Ar), 135.2 (CH Ar), 143.2 (CH

Ar), 144.4 (CH Ar), 156.2 (q, Gua). ν_{\max} (ATR)/cm⁻¹: 3237 (NH), 3115 (NH), 3057 (NH), 2587, 2390, 2331, 2164, 2032, 1658 (C=N), 1570, 1507, 1478, 1424, 1385, 1261, 1179, 1131, 1047, 1013, 933, 838, 810, 721, 687. HRMS (ESI⁺) m/z : [M + H]⁺ calcd for C₆H₉N₄ 137.0827. Found: 137.0829. Purity by HPLC: 99.2% (t_R = 2.19 min).

1-(Pyridin-3'-yl)-2-iminoimidazolidine Hydrochloride (11d): Procedure B. Clear, crystalline solid (98%). Mp 112–115 °C, decomposition. δ_H (400 MHz, DMSO-*d*₆): 3.69 (s, 4H, CH₂), 7.67 (app t, 1H, J = 6.6, Ar), 7.94 (d, 1H, J = 8.3, Ar), 8.59 (d, 1H, J = 4.4, Ar), 8.66 (s, 1H, Ar), 8.69 (br s, 2H, NH), 11.08 (br s, 1H, NH). δ_C (150 MHz, DMSO-*d*₆): 42.7 (2 CH₂), 127.1 (CH Ar), 137.4 (CH Ar), 138.1 (CH Ar), 140.1 (CH Ar), 135.7 (q Ar), 157.5 (q, Imi). ν_{\max} (ATR)/cm⁻¹: 3343 (NH), 3070 (NH), 3040 (NH), 2975, 2864, 2744, 2444, 2067, 1639 (C=N), 1608, 1556, 1514, 1468, 1420, 1366, 1339, 1328, 1284, 1252, 1190, 1089, 1046, 1021, 928, 885, 859, 815, 748, 671. HRMS (ESI⁺) m/z : [M + H]⁺ calcd for C₈H₁₁N₄ 163.0984. Found: 163.0987. Purity by HPLC: 99.2% (t_R = 4.00 min).

1-(6-Chloropyridin-3-yl)guanidine Hydrochloride (12c): Procedure B. White solid (92%). Mp 190–196 °C, clean melt. δ_H (600 MHz, DMSO-*d*₆): 7.59 (d, 1H, J = 8.5, Ar), 7.73 (br s, 4H, NH), 7.76 (dd, 1H, J = 8.5, 2.5, Ar), 8.33 (d, 1H, J = 2.5, Ar), 10.16 (br s, 1H, NH). δ_C (150 MHz, DMSO-*d*₆): 125.0 (CH Ar), 132.0 (q Ar), 136.4 (CH Ar), 146.3 (CH Ar), 147.4 (q Ar), 156.3 (q, Gua). ν_{\max} (ATR)/cm⁻¹: 3278 (NH), 3092 (NH), 3050 (NH), 2839, 2163, 2012, 1910, 1667 (C=N), 1632, 1603, 1584, 1454, 1417, 1362, 1287, 1266, 1132, 1106, 1029, 1010, 934, 873, 833, 745, 707. HRMS (ESI⁺) m/z : [M + H]⁺ calcd for C₆H₈N₄³⁵Cl 171.0437. Found: 171.0433. Purity by HPLC: 96.0% (t_R = 7.43 min).

1-(6-Methylpyridin-3-yl)guanidine Hydrochloride (13c): Procedure B. White solid (82%). Mp 171–172 °C, clean melt. δ_H (600 MHz, DMSO-*d*₆): 2.73 (s, 3H, CH₃), 7.86 (d, 1H, J = 8.7, Ar), 8.00 (br s, 4H, NH), 8.23 (dd, 1H, J = 8.7, 2.2, Ar), 8.72 (d, 1H, J = 2.2, Ar), 10.69 (br s, 1H, NH). δ_C (150 MHz, DMSO-*d*₆): 19.3 (CH₃), 127.6 (CH Ar), 132.8 (q Ar), 138.6 (CH Ar), 140.1 (CH Ar), 151.5 (q Ar), 156.3 (q, Gua). ν_{\max} (ATR)/cm⁻¹: 3275 (NH), 2894, 1677 (C=N), 1622, 1603, 1565, 1491, 1456, 1376, 1288, 1244, 1107, 1025, 875, 832, 798, 739, 716. HRMS (ESI⁺) m/z : [M + H]⁺ calcd for C₇H₁₁N₄ 151.0984. Found: 151.0980. Purity by HPLC: 99.7% (t_R = 3.16 min).

1-(5,6,7,8-Tetrahydroquinolin-3-yl)guanidine Hydrochloride (14c): Procedure B. White solid (87%). Mp 85–88 °C, clean melt. δ_H (600 MHz, DMSO-*d*₆): 1.78 (app t, 2H, J = 5.9, 5.5, CH₂), 1.86 (app t, 2H, J = 5.9, 5.5, CH₂), 2.85 (t, 2H, J = 6.1, CH₂), 2.97 (app t, 2H, J = 6.1, CH₂), 7.76 (br s, 4H, NH), 7.85 (s, 1H, Ar), 8.48 (s, 1H, Ar), 10.25 (br s, 1H, NH). δ_C (150 MHz, DMSO-*d*₆): 21.5 (CH₂), 21.7 (CH₂), 27.8 (CH₂), 29.1 (CH₂), 131.6 (q Ar), 135.9 (q Ar), 138.3 (CH Ar), 139.3 (CH Ar), 152.4 (q Ar), 155.6 (q, Gua). ν_{\max} (ATR)/cm⁻¹: 3274 (NH), 2893, 1676 (C=N), 1620, 1598, 1563, 1490, 1376, 1325, 1289, 1244, 1083, 1025, 904, 876, 831, 737, 716, 653. HRMS (ESI⁺) m/z : [M + H]⁺ calcd for C₁₀H₁₅N₄ 191.1297. Found: 191.1292. Purity by HPLC: 96.4% (t_R = 10.11 min).

1-(5,6,7,8-Tetrahydroquinolin-3'-yl)-2-iminoimidazolidine Hydrochloride (14d): Procedure B. White, crystalline solid (91%). Mp 122–126 °C, clean melt. δ_H (600 MHz, DMSO-*d*₆): 1.79 (app p, 2H, CH₂), 1.86 (app p, 2H, CH₂), 2.87 (app t, 2H, J = 6.1, CH₂), 3.01 (app t, 2H, J = 6.2, CH₂), 3.70 (br s, 4H, CH₂), 7.99 (s, 1H, Ar), 8.54 (s, 1H, Ar), 8.81 (br s, 2H, NH), 11.35 (br s, 1H, NH). δ_C (150 MHz, DMSO-*d*₆): 21.3 (CH₂), 21.4 (CH₂), 27.7 (CH₂), 28.3 (CH₂), 43.0 (2 CH₂), 132.7 (q Ar), 136.7 (CH Ar), 138.0 (CH Ar), 151.3 (q Ar), 158.1 (q, Imi), 164.6 (q Ar). ν_{\max} (ATR)/cm⁻¹: 3418 (NH), 3108 (NH), 3020 (NH), 2955, 2932, 2898, 2868, 2812, 2418, 2035, 1622 (C=N), 1560, 1504, 1445, 1418, 1322, 1262, 1215, 1087, 1027, 1000, 947, 932, 898, 826, 779, 729, 688. HRMS (ESI⁺) m/z : [M + H]⁺ calcd for C₁₂H₁₇N₄ 217.1453. Found: 217.1446. Purity by HPLC: 96.1% (t_R = 17.20 min).

1-[6-(*N*-Ethylamino)pyridin-3-yl]guanidine Hydrochloride (15c): Procedure B. White, crystalline solid (100%). Mp 120–124 °C, decomposition. δ_H (600 MHz, DMSO-*d*₆): 1.22 (t, 3H, J = 7.1, CH₃), 3.43 (q, 2H, J = 7.1, CH₂), 7.13 (d, 1H, J = 9.5, Ar), 7.67 (br s, 4H, NH), 7.75 (dd, 1H, J = 1.9, 9.5, Ar), 7.91 (d, 1H, J = 1.9, Ar), 9.17 (br s, 1H, NH, NHet), 9.81 (br s, 1H, NH). δ_C (150 MHz, DMSO-

d_6): 14.0 (CH₃), 37.3 (CH₂), 114.6 (CH Ar), 121.0 (q Ar), 135.3 (CH Ar), 142.4 (CH Ar), 152.3 (q Ar), 157.5 (q, Gua). ν_{\max} (ATR)/cm⁻¹: 3310, 3250 (NH), 3179 (NH), 3129 (NH), 3040 (NH), 2973, 2848, 2808, 2770, 1663 (C=N), 1605, 1582, 1502, 1439, 1376, 1336, 1302, 1273, 1230, 1166, 1103, 1055, 1021, 1005, 875, 858, 821, 781, 684. HRMS (ESI⁺) m/z : [M + H]⁺ calcd for C₈H₁₄N₅ 180.1249. Found: 180.1246. Purity by HPLC: 96.3% (t_R = 2.41 min).

1-(6-(Ethylamino)pyridin-3'-yl)-2-iminoimidazolidine Hydrochloride (15d): Procedure B. White, crystalline solid (95%). Mp above 210 °C, decomposition. δ_H (600 MHz, DMSO- d_6): 1.22 (t, 3H, J = 7.1, CH₃), 3.45 (q, 2H, J = 7.1, CH₂), 3.65 (s, 4H, CH₂), 7.15 (d, 1H, J = 9.4, CH₂), 7.76 (d, 1H, J = 9.4, Ar), 7.92 (s, 1H, Ar), 8.55 (br s, 2H, NH), 10.63 (br s, 1H, NH). δ_C (150 MHz, DMSO- d_6): 13.7 (CH₃), 37.0 (CH₂), 42.7 (2 CH₂), 113.9 (CH Ar), 121.5 (q Ar), 133.8 (CH Ar), 141.0 (CH Ar), 151.9 (q Ar), 159.0 (q, Imi). ν_{\max} (ATR)/cm⁻¹: 3199 (NH), 3057 (NH), 2861, 1674, 1619 (C=N), 1589, 1482, 1458, 1407, 1375, 1320, 1279, 1213, 1154, 1128, 1108, 1085, 1066, 1020, 1002, 989, 934, 835, 786, 745, 717, 657. HRMS (ESI⁺) m/z : [M + H]⁺ calcd for C₁₀H₁₆N₅ 206.1406. Found: 206.1401. Purity by HPLC: 97.9% (t_R = 3.21 min).

1-(5-Nitropyridin-2-yl)guanidine Hydrochloride (17c). To a solution of neutral 1-(5-nitropyridin-2-yl)guanidine (1.1 equiv, 133 mg, 1.39 mmol) and ^tBuOH (12 mL) was added finely ground NaOH (3.0 equiv, 151 mg, 3.79 mmol). The mixture was stirred for 30 min at rt after which 2-nitro-5-chloropyridine (1.0 equiv, 200 mg, 1.26 mmol) was added. Reflux at 120 °C was continued for 6 h. The resulting solution was extracted with ⁱPrOH/CH₂Cl₂ (20%, 4 × 30 mL) and washed with 2 M NaOH solution (30 mL). The organic extracts were combined, dried over MgSO₄, and concentrated in vacuo to give the neutral guanidine (153 mg, 67%). This was stirred at rt in a 1.25 M solution of HCl in CH₃OH (6.0 equiv, 5.98 mL, 7.47 mmol) for 3 h. Removal of solvent and purification by reverse phase chromatography (C-8 silica) with 100% H₂O as mobile phase yielded **16c** as yellow crystals (85%). Mp 93–95 °C, clean melt. δ_H (600 MHz, DMSO- d_6): 7.27 (d, 1H, J = 9.1, Ar), 8.49 (br s, 4H, NH), 8.62 (dd, 1H, J = 9.1, 2.7, Ar), 9.12 (d, 1H, J = 2.7, Ar), 12.17 (br s, 1H, NH). δ_C (150 MHz, DMSO- d_6): 113.7 (CH Ar), 135.0 (CH Ar), 140.3 (q Ar), 144.1 (CH Ar), 155.2 (q Ar), 156.0 (q, Gua). ν_{\max} (ATR)/cm⁻¹: 3426 (NH), 3318 (NH), 3185, 2924, 1687 (C=N), 1620, 1601, 1552, 1516, 1474, 1340, 1246, 1121, 1079, 1013, 984, 947, 864, 840, 758, 708. HRMS (ESI⁺) m/z : [M + H]⁺ calcd for C₆H₈N₅O₂ 182.0678. Found: 182.0679. Purity by HPLC: 96.8% (t_R = 18.97 min).

1-(5-Aminopyridin-2-yl)guanidine Hydrochloride (18c). To a solution of neutral 1-(5-nitropyridin-2-yl)guanidine (100 mg, 0.55 mmol) in CH₃OH (6 mL) was added 10% Pd/C (29 mg, 0.028 mmol, 5 mol %). The mixture was stirred under a hydrogen atmosphere (3 atm) for 7 h. It was then diluted with CH₃OH (30 mL), filtered through filter paper, and concentrated under reduced pressure. The unstable neutral guanidine was immediately converted to the hydrochloride salt by stirring the residue in a 1.25 M methanolic HCl solution (6.0 equiv, 2.6 mL, 3.30 mmol) for 3 h. Excess solvent and HCl were removed under reduced pressure, and the residue was dissolved in a minimum volume of H₂O. The aqueous layer was washed with CH₂Cl₂ (2 × 2 mL) and concentrated under reduced pressure to yield a red solid, which was purified by reverse phase chromatography (C-8 silica) with 100% H₂O as mobile phase. Recrystallization from CH₃OH/Et₂O afforded **18c** as a red solid (69%). Mp 200–202 °C, burned. δ_H (600 MHz, DMSO- d_6): 3.82 (br s, 2H, NH₂), 7.03 (d, 1H, J = 8.8, Ar), 7.56 (d, 1H, J = 8.8, Ar), 8.08 (s, 1H, Ar), 8.20 (br s, 4H, NH), 11.39 (br s, 1H, NH). δ_C (150 MHz, DMSO- d_6): 113.9 (CH Ar), 127.2 (CH Ar), 133.8 (q Ar), 137.5 (CH Ar), 143.7 (q Ar), 154.7 (q, Gua). ν_{\max} (ATR)/cm⁻¹: 3308 (NH), 2795, 2544, 2025, 1682 (C=N), 1627, 1602, 1560, 1488, 1396, 1287, 1252, 1226, 1137, 1099, 1033, 877, 825, 807, 731. HRMS (ESI⁺) m/z : [M + H]⁺ calcd for C₆H₁₀N₅ 152.0936. Found: 152.0934. Purity by HPLC: 97.4% (t_R = 4.84 min).

N-Phenyl-1,4-dihydroquinazolin-2-amine Hydrochloride (19i): Procedure D. White solid (93%). Mp 122–124 °C, clean melt. δ_H (600 MHz, DMSO- d_6): 4.75 (d, 2H, J = 5.2, CH₂), 7.04 (br s, 1H, Ar), 7.09 (br s, 1H, Ar), 7.14 (t, 1H, J = 7.3, Ar), 7.22 (t, 1H, J =

7.1, Ar), 7.30–7.33 (m, 1H, Ar), 7.34 (t, 2H, J = 7.3, Ar), 7.46 (d, 2H, J = 7.3, Ar), 8.21 (br s, 1H, NH), 9.84 (br s, 1H, NH). δ_C (150 MHz, DMSO- d_6): 42.9 (CH₂), 123.7 (q Ar), 123.8 (CH Ar), 124.8 (CH Ar), 128.3 (CH Ar), 128.6 (CH Ar), 129.0 (CH Ar), 129.5 (q Ar), 130.6 (q Ar), 133.1 (CH Ar), 139.7 (CH Ar), 181.5 (q, CN). ν_{\max} (ATR)/cm⁻¹: 3221 (NH), 2810, 2554, 1980, 1744, 1594 (C=N), 1534, 1494, 1452, 1380, 1343, 1313, 1265, 1121, 1093, 1029, 939, 835, 748, 694. HRMS (ESI⁺) m/z : [M + H]⁺ calcd for C₁₄H₁₄N₃ 224.1188. Found: 224.1194. Purity by HPLC: 96.4% (t_R = 28.55 min).

N-(Ethoxy)-1,4-dihydroquinazolin-2-amine Hydrochloride (19j): Procedure D. White solid (95%). Mp 139–140 °C, clean melt. δ_H (400 MHz, DMSO- d_6): 3.57 (t, 2H, J = 7.5, CH₂), 3.90 (t, 2H, J = 7.5, CH₂), 3.90 (br s, 1H, OH), 4.84 (d, 2H, J = 5.2, CH₂), 7.34–7.50 (m, 4H, Ar), 8.45 (br s, 1H, NH), 9.99 (br s, 1H, NH), 10.96 (br s, 1H, NH). δ_C (100 MHz, DMSO- d_6): 44.0 (CH₂), 30.9 (CH₂), 48.8 (CH₂), 123.6 (CH Ar), 127.8 (CH Ar), 128.8 (CH Ar), 129.1 (q Ar), 129.4 (CH Ar), 131.3 (q Ar), 170.1 (q, CN). ν_{\max} (ATR)/cm⁻¹: 2793, 2561, 2020, 1634 (C=N), 1580, 1494, 1455, 1343, 1292, 1244, 1127, 1071, 940, 873, 755, 679. HRMS (ESI⁺) m/z : [M + H]⁺ calcd for C₁₀H₁₄N₃O 192.1137. Found: 192.1143. Purity by HPLC: 97.3% (t_R = 19.96 min).

N-(2-Furanylmethyl)-1,4-dihydroquinazolin-2-amine Hydrochloride (19k): Procedure D. Tan solid (30%). Mp 50–52 °C, clean melt. δ_H (400 MHz, DMSO- d_6): 4.66 (s, 2H, CH₂), 4.84 (d, 2H, J = 4.6, CH₂), 6.29 (br s, 1 H, Ar), 6.40 (s, 1H, Ar), 7.37 (m, 1H, Ar), 7.38–7.40 (m, 2H, Ar), 7.47 (s, 1H, Ar), 7.59 (s, 1H, Ar), 8.31 (br s, 1H, NH), 8.39 (br s, 1H, NH). δ_C (100 MHz, DMSO- d_6): 38.4 (CH₂), 41.3 (CH₂), 108.8 (CH Ar), 111.1 (CH Ar), 116.0 (CH Ar), 124.8 (CH Ar), 126.7 (CH Ar), 129.0 (CH Ar), 133.8 (q Ar), 140.3 (q Ar), 143.6 (CH Ar), 152.4 (q Ar), 174.2 (q, CN). ν_{\max} (ATR)/cm⁻¹: 2834, 2574, 1623 (C=N), 1590, 1560, 1496, 1456, 1299, 1226, 1070, 1011, 939, 883, 753. HRMS (ESI⁺) m/z : [M + H]⁺ calcd for C₁₃H₁₄N₃O 228.1137. Found: 228.1146. Purity by HPLC: 97.6% (t_R = 27.95 min).

N-(*n*-Propyl)-1,4-dihydroquinazolin-2-amine Hydrochloride (19l): Procedure D. White solid (90%). Mp 80–82 °C, clean melt. δ_H (400 MHz, DMSO- d_6): 0.92 (t, 3H, J = 7.1, CH₃), 1.54 (m, 2H, CH₂), 3.27 (m, 2H, CH₂), 4.46 (s, 2H, CH₂), 7.02–7.09 (m, 2H, Ar), 7.19 (d, 1H, J = 7.2, Ar), 7.24 (t, 1H, J = 7.2, Ar), 8.32 (br s, 1H, NH), 8.79 (br s, 1H, NH), 10.82 (br s, 1H, NH). δ_C (100 MHz, DMSO- d_6): 11.0 (CH₃), 21.9 (CH₂), 40.8 (CH₂), 42.7 (CH₂), 123.9 (q Ar), 126.2 (CH Ar), 128.4 (CH Ar), 133.5 (CH Ar), 145.5 (q Ar), 151.8 (CH Ar), 166.9 (q, CN). ν_{\max} (ATR)/cm⁻¹: 3233 (NH), 2872, 2558, 1992, 1618 (C=N), 1555, 1496, 1456, 1382, 1333, 1291, 1213, 1179, 1064, 935, 837, 750. HRMS (ESI⁺) m/z : [M + H]⁺ calcd for C₁₁H₁₆N₃ 190.1344. Found: 190.1347. Purity by HPLC: 96.7% (t_R = 26.23 min).

N-(Ethoxy)-1,4-dihydroxyrido[2,3-*d*]azin-2-amine Hydrochloride (20j): Procedure D. Yellow solid (98%). Mp 235 °C, decomposed. δ_H (400 MHz, DMSO- d_6): 3.52 (br s, 2H, CH₂), 3.86 (br s, 2H, CH₂), 4.49 (br s, 2H, CH₂), 6.86 (s, 1H, Ar), 7.88 (s, 1H, J = 8.0, Ar), 7.94 (d, 1H, J = 4.0, Ar), 8.18 (br s, 1H, NH), 8.25 (br s, 1H, NH), 10.61 (br s, 1H, NH). δ_C (100 MHz, DMSO- d_6): 31.1 (CH₂), 43.5 (CH₂), 49.2 (CH₂), 112.9 (CH Ar), 134.0 (q Ar), 135.4 (CH Ar), 142.6 (CH Ar), 151.8 (q Ar), 182.4 (q, CN). HRMS (ESI⁺) m/z : [M + H]⁺ calcd for C₉H₁₃N₄O 193.1089. Found: 193.1083. Purity by HPLC: 97.7% (t_R = 2.56 min).

N-(Furan-2-ylmethyl)-1,4-dihydroxyrido[2,3-*d*]pyrimidin-2-amine Hydrochloride (20k): Procedure D. White powder (86%). Mp 181 °C, decomposed. δ_H (400 MHz, DMSO- d_6): 4.53 (s, 2H, CH₂), 4.59 (s, 2H, CH₂), 6.25 (s, 1H, Ar), 6.34 (s, 1H, Ar), 6.85 (app t, 1H, J = 8.0, 4.0, Ar), 7.53 (s, 1H, Ar), 7.79 (d, 1H, J = 8.0, Ar), 7.87 (d, 1H, J = 4.0, Ar), 8.11 (br s, 1H, NH), 8.39 (br s, 1H, NH), 8.48 (br s, 1H, NH). δ_C (100 MHz, DMSO- d_6): 41.1 (CH₂), 42.9 (CH₂), 107.8 (CH Ar), 110.9 (CH Ar), 112.5 (CH Ar), 123.5 (q Ar), 134.5 (CH Ar), 141.4 (CH Ar), 142.7 (CH Ar), 151.7 (q Ar), 152.5 (q Ar), 172.5 (q, CN). HRMS (ESI⁺) m/z : [M + H]⁺ calcd for C₁₂H₁₃N₄O 229.1098. Found: 229.1098. Purity by HPLC: 96.2% (t_R = 23.27 min).

N-(1,3-Benzodioxol-5-ylmethyl)-1,4-dihydroxyrido[2,3-*d*]pyrimidin-2-amine Hydrochloride (20m): Procedure D. White powder (26%). Mp 196 °C. δ_H (400 MHz, DMSO- d_6): 4.59 (br s, 2H,

CH₂), 4.62 (s, 2H, CH₂), 5.98 (s, 2H, CH₂), 6.76 (app t, 1H, *J* = 4.0, Ar), 6.87 (m, 2H, Ar), 6.87 (s, 1H, Ar), 7.74 (d, 1H, *J* = 4.0, Ar), 7.92 (d, 1H, *J* = 4.0, Ar), 8.07 (br s, 1H, NH), 8.33 (br s, 1H, NH), 8.49 (br s, 1H, NH). δ_C (100 MHz, CDCl₃): 42.5 (CH₂), 42.7 (CH₂), 101.1 (CH₂), 112.2 (CH Ar), 108.5 (CH Ar), 115.3 (q Ar), 120.8 (CH Ar), 131.3 (q Ar), 134.3 (CH Ar), 147.1 (CH Ar), 146.9 (q Ar), 152.6 (q Ar), 181.3 (q CN). HRMS (ESI⁺) *m/z*: [M + H]⁺ calcd for C₁₅H₁₅N₄O₂ 283.1195. Found: 283.1190. Purity by HPLC: 99.8% (*t*_R = 24.40 min).

■ ASSOCIATED CONTENT

📄 Supporting Information

Preparation and characterization of all starting amines and Boc-protected or neutral guanidine intermediates; spectroscopic and HPLC data of final hydrochloride salts; further details of pharmacological assays, calculated pharmacokinetic parameters, and molecular modeling. This material is available free of charge via the Internet at <http://pubs.acs.org>.

■ AUTHOR INFORMATION

Corresponding Author

*E-mail: rozasi@tcd.ie. Phone: +353 1 896 3731.

Notes

The authors declare no competing financial interest.

■ ACKNOWLEDGMENTS

B.K. is grateful to the HEA-PRTLI-4 (Ireland) for financial support and to Trinity College Dublin for a travel grant. C.M. is recipient of a predoctoral fellowship from the University of the Basque Country (UPV/EHU), Spain. This work was also supported by grants from the Basque Government (Grant IT616-13; SAIOTEK S-PE12UN033), the University of the Basque Country (Grant UFI 11/35), Ministry of Economy and Competitiveness (Grant SAF2013-48586-R), and the Instituto de Salud Carlos III, Centro de Investigación Biomédica en Red de Salud Mental, CIBERSAM.

■ ABBREVIATIONS USED

α₂-AR, α₂-adrenoceptor; α_{2C}-AR, subtype C α₂-adrenoceptor; α_{2A}-AR, subtype A α₂-adrenoceptor; NA, noradrenaline; [³⁵S]GTPγS, sulfur labeled guanosine 5'-O-[γ-thio]-triphosphate; PFC, prefrontal cortex; BDNF, brain-derived neurotrophic factor; EC₅₀, E half maximal effective concentration; UK14304, brimonidine; RX821002, 2-methoxyvidazoxan; aCFS, artificial cerebrospinal fluid; E_{max}, maximum possible effect; *P* or *p*, probability; *F*_{tr}, *F* value, treatment, between groups; *F*_i, *F* value, time, within groups; *F*_v, *F* value, treatment × time, interaction; SAR, structure–activity relationship; p*K*_{aH}, minus logarithm of the acid constant of a base; IMHB, intramolecular hydrogen bond; log *D*, logarithm of the distribution coefficient; CNS, central nervous system; NMR, nuclear magnetic resonance; Boc, di-*tert*-butyl dicarbonate; DFT, density functional theory; p*K*_i, minus logarithm of the dissociation constant; GPCR, G-protein-coupled receptor; GDP, guanine diphosphate; β₂-AR, β₂-adrenoceptor; TM, transmembrane; hERG, human ether-a-go-go-related gene

■ REFERENCES

- (1) The Global Burden of Disease: 2004 Update. WHO Press: Geneva, 2008.
- (2) Callado, L. F.; Meana, J. J.; Grijalba, B.; Pazos, A.; Sastre, M.; García-Sevilla, J. A. Selective Increase of α_{2A}-Adrenoceptor Agonist

Binding Sites in Brains of Depressed Suicide Victims. *J. Neurochem.* **1998**, *70*, 1114–1123.

(3) Fernandez-Pastor, B.; Meana, J. J. In Vivo Tonic Modulation of the Noradrenaline Release in the Rat Cortex by Locus Coeruleus Somatodendritic α₂-Adrenoceptors. *Eur. J. Pharmacol.* **2002**, *442*, 225–229.

(4) Devoto, P.; Flore, G.; Pani, L.; Gessa, G. L. Evidence for Co-Release of Noradrenaline and Dopamine from Noradrenergic Neurons in the Cerebral Cortex. *Mol. Psychiatry* **2001**, *6*, 657–664.

(5) Leonard, B. E. Neuropharmacology of Antidepressants that Modify Central Noradrenergic and Serotonergic Function: a Short Review. *Hum. Psychopharmacol. Clin. Exp.* **1999**, *14*, 75–81.

(6) Rodriguez, F.; Rozas, I.; Ortega, J. E.; Meana, J. J.; Callado, L. F. Guanidine and 2-Aminoimidazoline Aromatic Derivatives as α₂-Adrenoceptor Antagonists. 1: Toward New Antidepressants with Heteroatomic Linkers. *J. Med. Chem.* **2007**, *50*, 4516–4527.

(7) Rodriguez, F.; Rozas, I.; Ortega, J. E.; Erdozain, A. M.; Meana, J. J.; Callado, L. F. Guanidine and 2-Aminoimidazoline Aromatic Derivatives as α₂-Adrenoceptor Antagonists. 2. Exploring Alkyl Linkers for New Antidepressants. *J. Med. Chem.* **2008**, *51*, 3304–3312.

(8) Goonan, A.; Kahvedžić, A.; Rodriguez, F.; Nagle, P.; McCabe, T.; Rozas, I.; Erdozain, A. M.; Meana, J. J.; Callado, L. F. Novel Synthesis and Pharmacological Evaluation as α₂-Adrenoceptor Ligands of O-Phenylisouronium Salts. *Bioorg. Med. Chem.* **2008**, *16*, 8210–8217.

(9) Rozas, I. Improving Antidepressant Drugs: Update on Recently Patented Compounds. *Expert Opin. Ther. Pat.* **2009**, *19*, 827–845.

(10) Rodriguez, F.; Rozas, I.; Ortega, J. E.; Erdozain, A. M.; Meana, J. J.; Callado, L. F. Guanidine and 2-Aminoimidazoline Aromatic Derivatives as α₂-Adrenoceptor Ligands: Searching for Structure–Activity Relationships. *J. Med. Chem.* **2009**, *52*, 601–609.

(11) Muguruza, C.; Rodriguez, F.; Rozas, I.; Meana, J. J.; Uriguen, L.; Callado, L. F. Antidepressant-like Properties of Three New α₂-Adrenoceptor Antagonists. *Neuropharmacology* **2013**, *65*, 13–19.

(12) O' Donovan, D. H.; Muguruza, C.; Callado, L. F.; Rozas, I. Guanidine-based α₂-Adrenoceptor Ligands: Towards Selective Antagonist Activity. *Eur. J. Med. Chem.* **2014**, *82*, 242–254.

(13) Alaa-Eldin, F. N.; Kamel, A. M.; Clarimont, C. Improving the Decision-Making Process in the Structural Modification of Drug Candidates: Enhancing Metabolic Stability. *Drug Discovery Today* **2004**, *9*, 1020–1028.

(14) Williams, R. p*K*_a Values. http://research.chem.psu.edu/brpgrp/pKa_compilation.pdf.

(15) Marvin, version 6.1.0; ChemAxon: Budapest, Hungary, 2013; <http://www.chemaxon.com>.

(16) Kelly, B.; O' Donovan, D. H.; O' Brien, J.; McCabe, T.; Blanco, F.; Rozas, I. Pyridin-2-yl Guanidine Derivatives: Conformational Control Induced by Intramolecular Hydrogen-Bonding Interactions. *J. Org. Chem.* **2011**, *76*, 9216–9227.

(17) van der Waterbeemd, H.; Smith, D. A.; Jones, B. C. Lipophilicity in PK Design: Methyl, Ethyl, Futile. *J. Comput.-Aided Mol. Des.* **2001**, *15*, 273–286.

(18) Kim, K. S.; Qian, L. Improved Method for the Preparation of Guanidines. *Tetrahedron Lett.* **1993**, *34*, 7677–7680.

(19) Dardonville, C.; Goya, P.; Rozas, I.; Alsasua, A.; Martín, I.; Borrego, J. New Aromatic Iminoimidazolidine Derivatives as α₁-Adrenoceptor Antagonists: A Novel Synthetic Approach and Pharmacological Activity. *Bioorg. Med. Chem.* **2000**, *8*, 1567–1577.

(20) O'Donovan, D. H.; Kelly, B.; Diez-Cecilia, E.; Kitson, M.; Rozas, I. A Structural Study of *N,N'*-Bis-aryl-*N''*-acylguanidines. *New J. Chem.* **2013**, *37*, 2408–2418.

(21) Das, P.; Kumar, C. K.; Kumar, K. N.; Innus, M.; Iqbal, J.; Srinivas, N. Dithiocarbamate and CuO Promoted One-Pot Synthesis of 2-(*N*-Substituted)-Aminobenzimidazoles and Related Heterocycles. *Tetrahedron Lett.* **2008**, *49*, 992–995.

(22) Gaspari, P.; Banerjee, T.; Malachowski, W. P.; Muller, A. J.; Prendergast, G. C.; DuHadaway, J.; Bennett, S.; Donovan, A. M. Structure–Activity Study of Brassinin Derivatives as Indoleamine 2,3-Dioxygenase Inhibitors. *J. Med. Chem.* **2006**, *49*, 684–692.

(23) Pajouhesh, H.; Lenz, G. R. Medicinal Chemical Properties of Successful Central Nervous System Drugs. *NeuroRx* **2005**, *2*, 541–553.

(24) Kratz, J. M.; Schuster, D.; Edtbauer, M.; Saxena, P.; Mair, C. E.; Kirchbner, J.; Matuszczak, B.; Baburin, I.; Hering, S.; Rollinger, J. M. Experimentally Validated hERG Pharmacophore Models as Cardiotoxicity Prediction Tools. *J. Chem. Inf. Model.* **2014**, DOI: 10.1021/ci5001955.

(25) Ortega, J. E.; Fernández-Pastor, B.; Callado, L. F.; Meana, J. J. In Vivo Potentiation of Reboxetine and Citalopram Effect on Extracellular Noradrenaline in Rat Brain by α_2 -Adrenoceptor Antagonism. *Eur. Neuropsychopharmacol.* **2010**, *20*, 813–822.

(26) Eswar, N.; Marti-Renom, M. A.; Webb, B.; Madhusudhan, M. S.; Eramian, D.; Shen, M.; Pieper, U.; Sali, A. Comparative Protein Structure Modeling with MODELLER. *Current Protocols in Bioinformatics*; John Wiley & Sons, Inc.: New York, 2006; Supplement 15, pp 5.6.1–5.6.30.

(27) Aantaa, R.; Marjamaeki, A.; Scheinin, M. Molecular Pharmacology of alpha2-Adrenoceptor Subtypes. *Ann. Med.* **1995**, *27*, 439–449.

(28) Rasmussen, S. G. F.; Choi, H. J.; Rosenbaum, D. M.; Kobilka, T. S.; Thian, F. S.; Edwards, P. C.; Burghammer, M.; Ratnala, V. R.; Sanishvili, R.; Fischetti, R. F.; Schertler, G. F.; Weis, W. I.; Kobilka, B. K. Crystal Structure of the Human β_2 Adrenergic G-Protein-Coupled Receptor. *Nature* **2007**, *450*, 383–387.

(29) Hanson, M. A.; Cherezov, V.; Griffith, M. T.; Roth, C. B.; Jaakola, V. P.; Chien, E. Y.; Velasquez, J.; Kuhn, P.; Stevens, R. C. A Specific Cholesterol Binding Site Is Established by the 2.8 Å Structure of the Human beta2-Adrenergic Receptor. *Structure* **2008**, *16*, 897–905.

(30) Rasmussen, S. G.; DeVree, B. T.; Zou, Y.; Kruse, A. C.; Chung, K. Y.; Kobilka, T. S.; Thian, F. S.; Chae, P. S.; Pardon, E.; Calinski, D.; Mathiesen, J. M.; Shah, S. T.; Lyons, J. A.; Caffrey, M.; Gellman, S. H.; Steyaert, J.; Skiniotis, G.; Weis, W. I.; Sunahara, R. K.; Kobilka, B. K. Crystal Structure of the β_2 -Adrenergic Receptor–Gs Protein Complex. *Nature* **2011**, *477*, 549–555.

(31) Bissantz, C.; Kuhn, B.; Stahl, M. A Medicinal Chemist's Guide to Molecular Interactions. *J. Med. Chem.* **2010**, *53*, 5061–5084.

(32) Gyires, K.; Zadori, Z. S.; Torok, T.; Matyus, P. α_2 -Adrenoceptor Subtypes-Mediated Physiological, Pharmacological Actions. *Neurochem. Int.* **2009**, *55*, 447–453.

(33) Kalkman, H. O.; Loetscher, E. α_{2C} -Adrenoceptor Blockade by Clozapine and Other Antipsychotic Drugs. *Eur. J. Pharmacol.* **2003**, *462*, 33–40.

(34) Paxinos, G.; Watson, C. *The Rat Brain in Stereotaxic Coordinates*, 2nd ed.; Academic Press: Orlando, FL, 1986.

(35) Vogel, A. I.; Tatchell, A. R.; Furnis, B. S.; Hannaford, A. J.; Smith, P. W. G. *Vogel's Textbook of Practical Organic Chemistry*, 5th ed.; Longman Group UK Limited: Harlow, U.K., 1996; ISBN 0582462363.

(36) Gottlieb, H. E.; Kotlyar, V.; Nudelman, A. NMR Chemical Shifts of Common Laboratory Solvents as Trace Impurities. *J. Org. Chem.* **1997**, *62*, 7512–7515.